



Review

Catalytic Oxidation Process for the Degradation of Synthetic Dyes: An Overview

Rahat Javaid ^{1,*}  and Umair Yaqub Qazi ²

¹ Renewable Energy Research Center, Fukushima Renewable Energy Institute, National Institute of Advanced Industrial Science and Technology, AIST, 2-2-9 Machiikedai, Koriyama, Fukushima 963-0298, Japan

² Chemistry Department, College of Science, University of Hafr Al Batin, P.O Box 1803 Hafr Al Batin 31991, Saud Arabia; umairqazi@uhb.edu.sa

* Correspondence: rahat.javaid@aist.go.jp

Received: 26 March 2019; Accepted: 7 June 2019; Published: 11 June 2019



Abstract: Dyes are used in various industries as coloring agents. The discharge of dyes, specifically synthetic dyes, in wastewater represents a serious environmental problem and causes public health concerns. The implementation of regulations for wastewater discharge has forced research towards either the development of new processes or the improvement of available techniques to attain efficient degradation of dyes. Catalytic oxidation is one of the advanced oxidation processes (AOPs), based on the active radicals produced during the reaction in the presence of a catalyst. This paper reviews the problems of dyes and hydroxyl radical-based oxidation processes, including Fenton's process, non-iron metal catalysts, and the application of thin metal catalyst-coated tubular reactors in detail. In addition, the sulfate radical-based catalytic oxidation technique has also been described. This study also includes the effects of various operating parameters such as pH, temperature, the concentration of the oxidant, the initial concentration of dyes, and reaction time on the catalytic decomposition of dyes. Moreover, this paper analyzes the recent studies on catalytic oxidation processes. From the present study, it can be concluded that catalytic oxidation processes are very active and environmentally friendly methods for dye removal.

Keywords: advanced oxidation process; catalyst; fenton reaction; hydroxyl radical; sulphate radical; synthetic dyes; tubular reactors

1. Introduction

With an increasing world population, the demand for basic raw materials and concluding products is increasing exponentially. Global economic growth and industrial revolutions lead to speedy metropolitanization. According to an estimation, over 700 emerging pollutants such as the waste contaminants of petrochemicals, personal care, textile, and pesticides are being confirmed in the aquatic ecosystem of the European region [1–4]. Among these, the textile and dyeing industries are considered among the major sources of water contamination. In textile mills, two principal processes contribute to the release of dyes in the environment: one is from the cleaning of the dye tank following the preparation of the dye bath, and the other is from the draining of the dye bath after the dyeing process is complete [5]. Dyeing industries use large volumes of water and dyes. Approximately 8–20% unutilized dyes and auxiliary chemicals are discharged into the wastewater stream from textile industries [6]. Approximately 1–10% of pigments used in paper and leather industries are lost as waste. Thus, tons of dyes are discharged daily into the environment as aquatic waste [7]. The wastewater from these industries contains high levels of biochemical oxygen demand (BOD) and chemical oxygen demand (COD) [8,9]. The discharge of contaminated effluent without any treatment into

the environment creates various environmental threats, including depressed photosynthesis and aquatic plant demise [10]. Moreover, most of these dyes and their components are carcinogenic and mutagenic with harmful impacts on all living beings on the earth [11–13]. Even the presence of a small quantity of these compounds (less than 1 ppm) in water has adverse effects. Many countries have strict regulations on the release of wastewaters from textile industries without proper processing to remove the excessive concentrations of color and COD [14].

Synthetic dyes are more resistant and difficult to degrade completely using photolysis, biological and chemical decomposition, and other ordinary approaches. Different technologies are accessible to decrease the absorption of these dyes into the environment such as ion exchange, chemical sedimentation, electrochemical reduction, membrane process, and adsorption [15–17]. All these available technologies have limitations, including the inefficient mineralization of the synthetic dyes, dense solution disposal, high energy consumption, high operation costs, and the excessive production of sludge, etc. [18–20]. Therefore, there are intensive demands for highly efficient and progressive newer technologies for the complete removal of the contaminants from the aquatic environment [21,22]. Among new alternative technologies for wastewater treatment, one effective technique is advanced oxidation processes (AOPs), which can be used to convert toxic and resistant chemicals into environmentally benign minerals. The highly efficient degradation of wastewater compounds is achievable by adopting a direct oxidation approach, but the requirement of severe operation conditions (e.g., high temperature and pressure) for the degradation of selected compounds increases the overall process cost [23–27]. Catalytic oxidation is one of the most efficient AOPs, based on the active radicals produced during the reaction in the presence of a catalyst at relatively mild reaction conditions. The catalytic process is based on the formation of strong oxidizing radicals that have dominant abilities to eliminate most of the pollutants present in wastewater. The main objective of the catalytic oxidation process is the conversion of synthetic dyes to benign products [28]. In catalysis, since the processes are performed on the surface of the catalyst, density, porosity, surface area, higher activity and selectivity for an oxidizing radical generation, stability, homogeneity, and low cost become the pivotal factors that affect the overall reaction performance.

This review paper addresses the problems of synthetic dyes and various catalytic degradation techniques available for their efficient mineralization. The main focus of this study is to discuss current research progress and general surveys either in the form of new process developments or the improvement of already existing technologies to accomplish the removal of synthetic dyes by adopting a catalytic oxidation route. Recent developments in the hydroxyl radical-based oxidation process are evaluated, and a critical analysis of various Fenton processes, possible mechanistic approaches, feasible conditions, the effect of various factors, advantages, and disadvantages are summarized. Non-iron metal catalysts and the application of thin metal catalyst-coated tubular reactors have been described in detail. In addition, the sulfate radical-based catalytic oxidation technique has also been summarized.

2. Toxic Effects of Dispersed Synthetic Dyes

A dye is a colored organic substance with a common property to absorb visible light and ability to attach strongly with fiber by means of chemical or physical bonding between the groups of fiber and dyes. Commercially, dyes should be quickly responsive to visible light, rubbing, and water. Not all color substances are dyes or dyestuff because color is a physiological perception concerned with light wavelengths hitting the retina of our eyes. The perception of color is only formed when a molecule absorbs the specific wavelength of light in the visible region of the electromagnetic spectrum and transmits or reflects the other wavelengths [29]. Dye molecules are made up of two main components—chromophores and auxochromes. The presence of chromophores in the structure is responsible for color formation while auxochromes work as an additive and make the molecule soluble in water as well as develop a strong attachment with fibers [30–32]. Hence, thousands of different dyes are synthesized for potential commercial applications by the alteration in molecular

structure. Generally, dyes can be classified based on their chemical structure as well as the existence of specific chromophores.

The dyes are made up of the by-products of petroleum and the minerals. Various kinds of synthetic dyes are commonly used industrially and classified as azo dyes, anthraquinone, triphenylmethane, phthalocyanine, indigo, and sulfur dyes. Most often, the fundamental chemical structure contains chromophores such as $-C=C-$, $-C=O$, $-N=N-$, $-NO_2$, $-C=N$, and quinonoid structural rings which are authoritative for the absorption of light in the wavelength of visible range. The classification of each compound is related to the existence of a particular functional group attached with the fundamental structure known as auxochromes, such as halogens, $-CO_2H$, $-COR$, $-SO_3H$, $-CH_3CO-$, $-CH_3$, and $-NH_2$ [33]. Figure 1 presents the fundamental structures of some synthetic dyes.

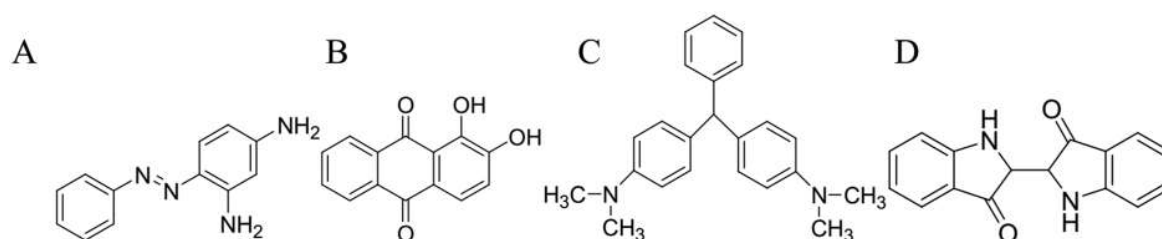


Figure 1. The fundamental structure of some synthetic dyes. (A) Azo dye (chrysoidine), (B) anthraquinone (alizarine), (C) triphenylmethane (malachite green), (D) indigo dye (indigo) [33].

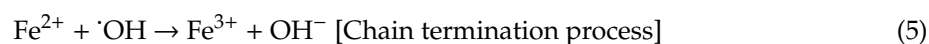
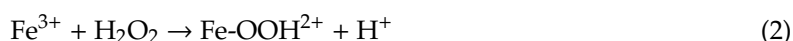
Over 10,000 different types of commercial pigments and dyes are produced annually [34]. Because of their variety of colors, easy utilization, and good stability, synthetic dyes are applied more frequently in industries [35]. The adoption of synthetic dyes spread during the industrial revolution and became a crucial part of the textile, paper, and food industries [36]. The annual production of dyes is reported as over 900,000 metric ton [37], and most of them are used in the textile industry. Over 70% of dyes are synthetic and sold out with their common or commercial names [38,39]. This could be the reason that most of the workers are not aware of their fundamental chemistry and ready to face the severe toxic effects due to the lack of proper handling for degradation. Every year, textile industries discharge an enormous quantity of colored substances into neighboring water without proper treatment, causing major environmental pollution. The industrial revolution means the construction of more industry with the usage of a huge quantity of dyes, increasing the toxicity in the whole ecosystem. Synthetic dyes keep their xenobiotic and wayward nature, resulting in an extensive toxic effect on life. Textile industrial discharge contains a large amount of synthetic dyes along with toxic metal contents which enhance the BOD, COD, and the pH of the surrounding water resources [40,41]. When the dye-containing wastewater is mixed with clean water, it unbalances the recommended level of organic and inorganic parameters. Mixing colored material into the water decreases sunlight penetration deep into the water and affects the whole water ecosystem. The existing toxic compounds of synthetic dyes in water are absorbed by fish and all other living animals in the water. When human eat these poisonous fish, they become affected by the toxic substances, causing many diseases such as cramps, mental disorder, hypertension, etc. Synthetic dyes containing benzidine-based structures are reported as carcinogenic, causing a severe toxic effect on human bladder [42]. Synthetic dyes can easily dissolve in water and penetrate the skin, causing allergic reactions, cancer, and eye irritation [42]. Table 1 summarizes various synthetic dyes and their hazardous effects.

Table 1. Selected synthetic dyes commonly used in the textile industry: their types, applications, and hazardous effects.

Dye Pollutant	Application	Hazardous Effect	References
Aniline Yellow or 4-phenylazoaniline	Chemical industry, printer's ink, intermediate for dye synthesis	Induces liver and epidermal tumors, high hepato-carcinogenicity to male mouse	[43,44]
Benzamine (BZ)-based azo dye	Chemical industry	Carcinogenic effect on human urinary bladder and reported tumorigenic effect on laboratory animals	[45]
o-Aminoazotoluene (C.I. Solvent Yellow 3)	Food and chemical industry	Tumors in urinary bladder, gall bladder, lung, and live	[46]
Methyl Yellow (Butter Yellow) and derivatives	Chemical, food and textile industry	Highly toxic cancer-causing agent	[47]
Reactive Brilliant Red	Textile, paint industry	Inhibit function of human serum albumin, may react to body protein or enzyme	[48]
Sudan azo dye (1-phenylazo-2-naphthol)	Petrochemical, textile and food industry	Carcinogenic in nature	[49]
Benzidine and its congener	Chemical industry	Carcinogenic to human urinary bladder, pancreas, liver, gallbladder, bile duct, lung, large intestine, stomach and renal cell	[50]
Direct Blue 15 (dimethoxybenzidine-based dye)	Biological and staining applications	Poisonous effect and mutagenicity in reduction process, carcinogenic	[42,51]
p-phenylenediamine (p-PDA)	Hair dye, personal care	Possibility of bladder cancer and skin allergy	[52]
p-Nitroaniline	Dyes intermediate, antioxidants, pharmaceuticals, corrosion inhibitor, petrochemical	Mutagenic, human carcinogen and induces tumors	[53]
Acid Violet 7	Food, paint, paper, cosmetic, and especially in textile industries	Chromosomal aberration, acetylcholinesterase activity inhibition, membrane lipid peroxidation	[54]
o-Toluidine (2-methylaniline)	Intermediate for dye, rubber, and pharmaceuticals	Urinary bladder cancer	[55]
2, 4-Diaminotoluene	Dye industry	Induces tumor in rats and mice, potential human carcinogenic effect	[56]
Malachite Green	Dye stuff in silk, leather, paper and antimicrobial in aquaculture	Carcinogenic, mutagenic, chromosomal fractures, respiratory toxicity	[57]
2-Nitro-p-phenylenediamine	Chemical and pharmaceutical	Reported carcinogenic for female mice	[58]
2-Amino-4-nitrophenol	Cosmetic industry	Causes renal tubular cell hyperplasia	[59]
4-Nitro-o-phenylenediamine	Hair dye, cosmetic industry	Carcinogen to humans	[60]
Reactive Black 5 (sulfonated azo dye)	Color and dye industry	Restrict nitrogen use efficiency of plant, decrease the urease activity, carcinogenicity	[61–63]
o-Phenylenediamine (o-PDA)	Pharmaceutical, cosmetic products and corrosion inhibitor	Genotoxic, asthma, gastritis, rise in blood pressure, vertigo, tremors, and comas	[64]
Disperse Red 1 and Disperse Red 13	Textile industry	Mutagenic to salmonella with possibility on human beings, affecting the activity and composition of microbial communities	[65–67]
m-Phenylenediamine (m-PDA)	Dye component, additive for resin, coatings, polymers, cosmetic industry	Oxidation products are highly mutagenic	[68]
Congo Red	Cotton dyeing, textile industry	Carcinogenic and mutagenic	[69]
Nitro-group with monocyclic aromatic amines	Various chemical industries	Likely to be carcinogenic	[70]

3. Fenton Reaction

H.J. Fenton was the first to report the famous Fenton reaction in 1894 and illustrated the oxidation process utilizing hydrogen peroxide (H_2O_2) as oxidant and iron (Fe) as a catalyst in the presence of acidic (H^+) medium [71]. The chemistry of the Fenton reaction has been explained comprehensively in many published review articles [72,73]. The reaction mechanism of the Fenton oxidation reaction is a little complex [74], and various parameters influence the efficiency of the overall process. In general, the Fenton oxidation process starts with the generation of a hydroxyl free radical ($\cdot\text{OH}$) [75,76]. Hydroxyl radicals are one of the most active oxidants and can react 10^6 – 10^{12} times faster than ozone depending on the substrate to be degraded [77–79]. The steps involved in the Fenton reaction are described as below (Equations (1)–(7)), and Equation (1) is the chain initiation process [80,81].

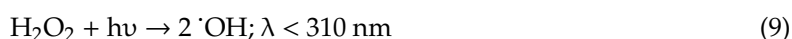
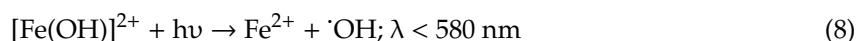


An acidic medium is required for the generation of hydroxyl radicals, and pH 3 is usually considered as the optimum condition for the Fenton oxidation reaction [82–86]. The formation of a large amount of ferric hydroxide precipitation is observed above pH 4, which decreases the efficiency of the process for dye degradation [87].

The Fenton reaction can be classified into two broad categories—homogeneous and heterogeneous processes. In homogeneous processes, iron species are in the same phase as the reactants and there is no limitation for mass transfer. Sludge formation with high iron contents, the deactivation of iron because of complex formation and a specific pH range (2.0–4.0) dependency are considered as the significant shortcomings of the homogeneous process. All these drawbacks can be conquered by the functionalization of the heterogeneous catalytic approach [88,89]. In heterogeneous catalysis, iron is sustained within the catalytic structure and can efficiently stimulate the degradation of recalcitrant materials without the formation of ferric hydroxide sludge. Based on the current research progress and investigations, three feasible mechanistic routes have been suggested to illustrate the heterogeneous catalytic Fenton reactions [90–96]. According to the first route, iron is percolated to the reaction solution and stimulates H_2O_2 using a homogeneous pathway. Another approach is chemisorption of the investigative molecules on the surface of the catalyst, whereas the third approach is the decomposition of H_2O_2 into hydroxyl radicals. Recent research progress reports have shown that heterogeneous catalysis is more competent than homogeneous catalysis for the degradation of synthetic dyes in wastewater [97]. Additionally, heterogeneous catalysis is more beneficial as: (1) the catalyst is easy to use and store, precisely recovered, and has the feasibility to reuse, (2) can be used at a wide range of pHs, and (3) can avoid the generation of ferric hydroxide precipitation. To enhance reaction performance, complexing agents such as nafion, zeolite, activated charcoal, clay, resin, silica have been used as supporting material for Fe [98–106]. Various types of Fenton processes are accessible to use such as photo-Fenton, electro-Fenton, photo-electro Fenton, sono-Fenton, sono-photo Fenton, and sono-electro Fenton processes [107,108]. Some of these are briefly described below.

3.1. Photo-Fenton Process

The improved form of the conventional Fenton oxidation reaction in the presence of UV–visible light below 600 nm wavelength is called the photo-Fenton reaction [109]. The involvement of UV–visible light provides two additional routes for the release of hydroxyl radicals, enhancing the degradation rate of dye pollutants [110]: (i) the photoreduction of Fe^{3+} to Fe^{2+} ions as shown in Equation (8) [111,112] and (ii) peroxide photolysis via shorter wavelengths (Equation (9)). The photo-generated ferrous ions enter the Fenton reaction to produce hydroxyl radicals. Therefore, the oxidation rate of the photo-Fenton process is higher than the Fenton process without using UV–visible light [113]. Moreover, the iron utilization and resultant sludge formation are comparably much reduced in photo-Fenton reaction [114].



In recent years, several reviews have been published on the applications of photo-Fenton processes for the removal of various kinds of organic pollutants present in wastewater [115,116]. The researchers have described many factors affecting the performance of the photo-Fenton process, including the type of light source, the power of the lamp, the structure of the reactor, metal concentration and H_2O_2 , etc. Among these factors, power and the source of light play an important role in determining the efficiency of the reaction [117,118]. Conventional UV lamps are used as a light irradiation source available as low-, medium-, and high-pressure mercury arc lamps. There are some disadvantages related to mercury lamps such as being hazardous, easy to break, after-use disposal, short working shelf life and the possibility of gas leakage because of high thermal stress on the glass. The risks are higher when medium- and high-pressure UV lamps are used, which are operated at a high temperature range of 600 to 900 °C [119]. Much research is demonstrated to overcome these disadvantages. For this purpose, sunlight irradiation has been introduced as a replacement for mercury lamps at the laboratory scale for the potential applications of photo-Fenton processes [120,121]. Solar generative photo-Fenton reactions have demonstrated high performance, achieving a high degree of mineralization as well as a level of performance up to 90% within a short reaction time [122]. The pH of the solution is another important parameter affecting the performance of the photo-Fenton process, as it strongly influences the complex formation or leaching of the catalyst [123].

The Photo-Fenton process was reported as a comparatively efficient method for the degradation of various synthetic dyes [124–126]. For example, among many advanced oxidation processes applied for the degradation of RB-19 dye, the photo-Fenton process was the most efficient method, showing 94.5% dissolved organic carbon and 99.4% total color removal [127,128].

3.2. Electro-Fenton Process

In recent years, electrochemical technology has gained much attention for the removal of wastewater pollutants. Many research articles are available that give a detailed overview of the electro-Fenton process for the degradation of synthetic dyes in wastewater [129,130]. There are notable advantages of the electrochemistry, including energy efficiency, versatility and environmental suitability as the electron and main-stream reagents are clean. Hence, by coupling the electrochemistry with the Fenton process, the oxidation efficiency can be significantly improved [131]. The electro-Fenton oxidation process consists of either adding Fe^{2+} or reducing Fe^{3+} electrochemically along with the simultaneous production of H_2O_2 from the reduction of O_2 on the electrodes [131]. Hydrogen peroxide is electrogenerated in acidic solutions by the two-electron reduction of oxygen on the cathode surface according to Equation (10) [132].



In comparison with the conventional Fenton process, the major benefit of this indirect electro-oxidation approach is the higher degradation rate of the organic pollutants due to the continuous transformation of the Fe^{3+} to Fe^{2+} at the cathode according to Equation (11) [133].



Fe^{2+} reacts with H_2O_2 to form active hydroxyl radicals in the aqueous medium. A continuous transformation of Fe^{3+} ensures the presence of sufficient Fe^{2+} ions which efficiently produce hydroxyl radicals, resulting in the higher degradation rate of the synthetic dyes [134]. Recently, a new technique was introduced for the electro-Fenton process in which a reduced graphene oxide (RGO) was electrochemically deposited on the surface of carbon felt and high performance was observed in the elimination of dyes, better stability and increased H_2O_2 formation. Table 2 summarizes the studies on the degradation of dyes by the electro-Fenton process.

Table 2. Degradation of dyes by an electro-Fenton process in various studies.

Dye Pollutant	References
Direct Orange 16	[135]
Acid Red 14	[136]
Basic Blue 3	[137]
4-Amino-3-hydroxy-2-p-tolylazo-naphthalene-1-sulfonic acid	[138]
Alizarin red	[139]
Yellow 52	[140]
4-Nitrophenol	[141]
Methyl Orange	[142]
Orange G	[143]
Rhodamine B	[144]
Lissamine Green B	[145]
Azure B	[145]
Reactive Black 5	[146]
Reactive Red 120	[147]
Orange II	[148]

3.3. Sono-Fenton Process

In recent years, ultrasonic waves have been employed for the degradation of highly contaminated wastewater. Ultrasonic is a sound wave with a frequency of approximately 20 kHz or above, which is greater than the upper limit of the human hearing range. The use of ultrasonic energy creates alternating expansion and compression cycles. The expansion cycles of ultrasonic waves result in acoustic cavitation in the form of microbubbles [149]. Later on, these microbubbles build up to a certain size and collapse fiercely during the compression wave cycle, resulting in several hundreds of atmospheric pressure and a several thousand Kelvins of temperature that could be up to the range of 1000 atm and 5000 K, respectively [150,151]. This energy dispensation phenomenon of bubble creation and collapse is called cavitation or the cold boiling process. Although these intense conditions live for a short interval, the degradation of organic pollutants is achieved either by pyrolytic cleavage or the generation of hydroxyl radicals. Under these vigorous conditions, highly reactive species such as hydroxyl ($\cdot\text{OH}$) and hydrogen ($\text{H}\cdot$) radicals are formed as described in Equations (12)–(15) [25–27,76,77]. This sono-chemical oxidation process creates an oxidative environment by the implementation of ultrasonic waves in the aqueous phase.





The combination of the ultrasonic and Fenton processes exhibits synergistic effects towards the degradation of organic pollutants because of the common fundamental oxidation mechanism [152, 153]. The mechanism involves the reaction of H_2O_2 with Fe^{2+} ions to generate active hydroxyl radicals similar to the Fenton process, whereas the resulting Fe^{3+} ions react with H_2O_2 to generate an intermediate iron complex which dissociates into Fe^{2+} and $\cdot\text{OOH}$ under the influence of ultrasound conditions as shown in Equation (16).



These Fe^{2+} ions further react with H_2O_2 , resulting in the production of hydroxyl radicals. Therefore, the sono-Fenton process generates a higher concentration of hydroxyl radicals than that produced in the absence of ultrasonic waves. Hence, the combination of the ultrasonic and Fenton system ($\text{Fe}^{2+}/\text{H}_2\text{O}_2$) is favorable and widely studied in detail in the literature [154]. From the literature, the sono-Fenton process is summarized as the high-performance process in terms of reaction rate and H_2O_2 usage. The self-production of oxidant species is favorable to overcome the extra cost of H_2O_2 . However, the high energy consumption of ultrasonic systems restricted the implementation of sono-Fenton system-based technologies. The degradation of various dyes by sono-Fenton and sono-photo-Fenton systems are described in Table 3.

Table 3. Degradation of wastewater pollutants by sono-Fenton and sono-photo-Fenton processes.

Dye Pollutant	References
Methylene Blue and Congo Red dyes	[155]
Reactive Blue 69	[156]
Aromatic Amines	[157]
Reactive Blue	[158]
Cephalexin	[159]
Non-volatile organic compound, dyes, Carbofuran	[160]
Bisphenol A	[161]
5-Fluorouracil	[162]
Nitrobenzene	[163]
Rhodamine B dye	[164]
Azure B	[165]

4. Non-Iron Metal Catalysts for Hydroxyl Radical-Based Oxidation

As the Fenton reaction using an iron-based catalyst has a significant drawback of a very narrow acidic pH region to attain the efficient decomposition of dyes [166], researchers focused on developing non-iron metal catalysts to overcome these shortcomings. It is suggested in various research works that transition metals other than iron, existing in at least two oxidation states such as Cu, Ru, Mn, Ag, and Co, can catalyze the formation of hydroxyl radicals from H_2O_2 [166–170]. There have been reports on the use of the colloidal nanoparticles of Au, Ag, and Pd for the degradation of methylene blue dye [171,172]. Among heterogeneous non-iron catalysts, $\text{Cu}/\text{Li}_2\text{O}/\gamma\text{-Al}_2\text{O}_3$ [173], TiO_2 nanoparticles on foamed polyethylene sheets [174], $\text{NiO}/\text{Al}_2\text{O}_3$ [175], etc. have also been applied to attain the efficient degradation of synthetic dyes in wastewater. Heterogeneous catalysts are considered more efficient and environmentally benign for catalytic application.

Salem et al., applied the Cu–ethylenediamine complex, supported on clay montmorillonite K10, as a heterogeneous catalyst to degrade acid blue 29 (AB29) dye, using H_2O_2 as an oxidant [176]. Almost 88.2% of the decolorization was obtained at 40 °C within a reaction time of 18 min. The authors also reported the influential role of the concentrations of the reactants and the temperature on

the efficiency for dye decomposition. The efficient Cu catalyzed decolorization of the dye solution was attributed to the formation of peroxo intermediates and hydroxyl radicals which acted as active oxidants to degrade AB dye.

Xaba et al. synthesized Pt nanoparticles in different sizes supported on mesoporous Co_3O_4 and applied them to attain the catalytic oxidative degradation of methylene blue (MB) dye, with H_2O_2 as an oxidant [177]. The highly efficient degradation of MB was achieved at ambient temperature conditions. Like other researchers, the authors reported different factors, including temperature, the concentration of dye, and H_2O_2 , affecting catalytic activity for the dye decomposition process. An increase in temperature and H_2O_2 concentration resulted in a significant incline in catalytic activity, while declining activity occurred on increasing the initial concentration of dye in the reactant stream. Amini et al. fabricated a MgAl-LDH-supported polyoxomolybdate catalyst for the degradation of methylene blue (MB) and rhodamine B (RB) dyes separately [178]. The catalyst showed higher activity in the presence of H_2O_2 as an oxidant, giving almost 100% degradation of MB and RB within a reaction time of 60 and 80 min, respectively, at ambient conditions. The efficiency for the catalytic degradation of both of the dyes increased dramatically on the increasing concentration of H_2O_2 . In contrast to iron-based catalysts, the alkaline medium was found to be more suitable to attain higher activity of the catalyst.

Among various supports, zeolites have also been recognized as an effective support for catalyst synthesis. Ag and Co ion-exchanged Y-type zeolites were synthesized and applied by Alekhina et al. for the catalytic degradation of carmoisine as an example of azo dyes [166]. They observed the highest oxidative degradation of dye using H_2O_2 , specifically for CoNaY catalyst in a slightly alkaline medium. On continuing their research on metal ion-exchanged zeolites, in another paper, Alekhina et al. compared the catalytic activities of Fe or Co ion-exchanged HY and NaY zeolites for the decomposition of carmoisine dye at 60 °C [170]. The authors also studied the effect of catalyst preparation conditions on the efficiency of the reaction. According to their findings, the complete decolorization of the carmoisine solution was attained in alkaline and weakly acidic media using CoNaY as a catalyst. Whereas, FeHY as a catalyst was mostly effective in a weakly acidic medium. Hence, it can be suggested, by considering all the above mentioned studies on different catalysts, that suitable reaction conditions to attain efficient activity for dye decomposition depend on the type of metal and support material as well as on the methods used for catalyst preparation.

5. Metal-Coated Tubular Reactors

We developed tubular reactors with inner walls coated with a thin metal catalyst layer and applied them to attain the efficient decomposition of synthetic dyes using high-pressure high-temperature water (HPHT- H_2O) as a reaction medium [179,180]. Microtubular reactors offer advantages including a simple flow reaction system, excellent mass, and heat transfer properties, a large surface-to-volume ratio, and an enhanced reaction rate [181–184]. Non-catalytic flow reaction processing using HPHT- H_2O has also been applied for the degradation of dyes [182–185]. The properties of water vary on increasing temperature and pressure from a polar liquid to an approximately nonpolar fluid above critical temperature (374.8 °C) and pressure (22.13 MPa) conditions. HPHT- H_2O provides advantages including a high thermal reaction rate, better dissolution of organic matters, low viscosity, excellent transport properties, etc. [185–188]. These properties of HPHT- H_2O make it a good alternative for various reaction mediums. The application of a tubular reactor with inner walls coated with a thin layer of the metal catalyst using HPHT- H_2O as a reaction medium not only provides the advantages of catalytic wet oxidation but also of HPHT- H_2O which ensures the complete decomposition of synthetic dyes in a short residence time. Here, we will summarize the experimental setup and the results of this novel approach for the complete decomposition of synthetic dyes using a catalytic tubular reactor and HPHT- H_2O as reported in our published papers [179,180].

The method for fabrication of catalytic tubular reactor is described in our various publications in detail [189–193]. Here, we provide a brief description. An Inconel (nickel alloy) tube (o.d. 1.6 mm,

i.d. 0.5 mm, length 1000 mm) was used as reactor with an inlaid TiO_2/Ti layer acting as a support for metal deposition. A thin layer of Pd as catalyst metal was coated on the inner walls of the reactor by an electroless plating technique. An electroless plating solution containing Pd precursor salt and reductant was continuously passed at constant temperature and flow rate to attain a thin deposited layer of Pd on the inner walls of the tubular reactor. The plating solution, after passing through the reactor, was analyzed by inductively coupled plasma-atomic emission spectroscopy (ICP-AES) to measure the amount of Pd deposited. Oxidation of the Pd surface to PdO was carried out by flowing air through the reactor at $750\text{ }^\circ\text{C}$ for 2 h. This PdO-coated catalytic tubular reactor provided a remarkably high surface area-to-volume ratio of $0.8 \times 10^4\text{ m}^2\text{ m}^{-3}$ [179,180]. Figure 2 presents the schematic diagram of the catalyst-coated tubular reactor (2a) and the experimental setup of the flow system (2b) [179]. Orange II dye in aqueous hydrogen peroxide (H_2O_2) solution was mixed with pre-heated water in the mixer and then passed continuously through the reactor at set temperature and pressure conditions. The solution from the reactor was analyzed for the removal of chemical oxygen demand (COD) and metal leaching. Continuous passage of the reactants mixed with HPHT- H_2O from a reactor without metal coating resulted in 22.5% COD removal at $200\text{ }^\circ\text{C}$ and 10 MPa gauge pressure, whereas, the application of a PdO-coated tubular reactor resulted in dramatically enhanced COD removal of 84.0% at the same reaction conditions. As reported by other researchers, the complete decomposition of synthetic dyes by oxygen or H_2O_2 requires much higher temperatures (above $400\text{ }^\circ\text{C}$) and longer reaction times (in minutes) [194]. Whereas, in our Pd catalyzed system, hydroxyl radicals generated by the catalytic decomposition of H_2O_2 [195–197] acted as a strong oxidant to destruct the stable aromatic ring of Orange II dye. Temperature played a vital role to attain higher efficiency for the catalytic decomposition of dyes, while the change in pressure did not notably affect catalytic activity. The almost complete removal of COD was obtained in a very short residence time of 4 s. Moreover, no leaching of metal was observed [179]. The initial concentration of the dye in the reactant stream also affected the rate of dye decomposition.

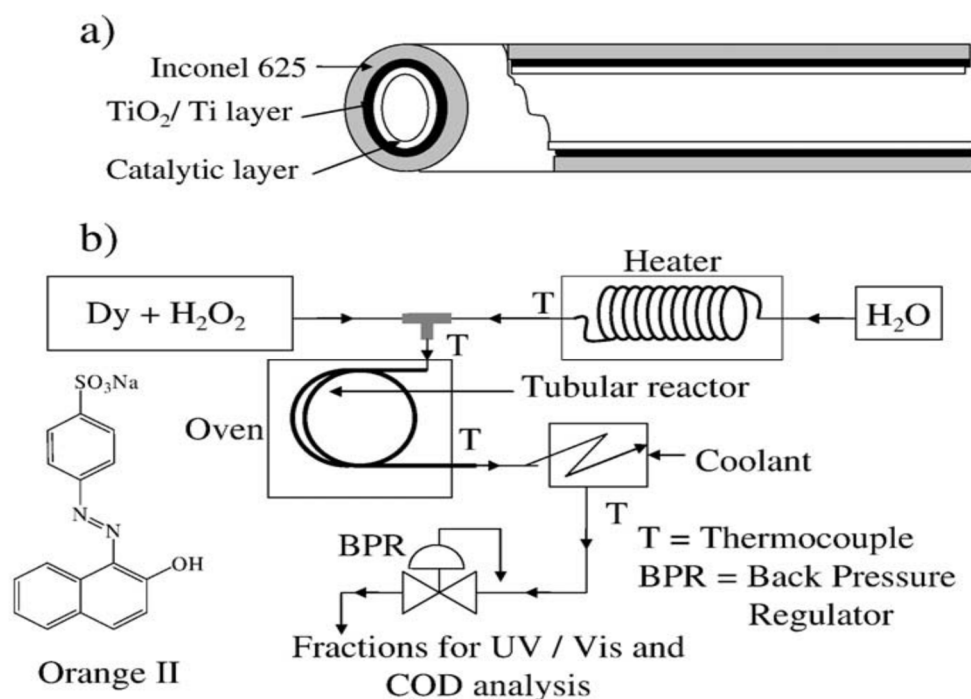


Figure 2. (a) Configuration of the catalyst-coated tubular reactor; (b) diagram of the HPHT- H_2O flow reactor system [179].

In another paper, we applied a catalytic tubular reactor using HPHT- H_2O to decompose Remazol Brilliant Blue R (RBBR) as another example of synthetic dyes. RBBR is one of the most important

synthetic dyes frequently used in the textile industry and as a starting material in the production of polymeric dyes. Figure 3 is adapted from our published paper [180]. Figure 3a shows the schematic diagram of a tubular reactor coated with a thin layer of the metal catalyst. The scanning electron microscopy (SEM) image (Figure 3b) presents the longitudinal section of the tubular reactor with thoroughly coated inner walls with the thin Pd layer. The magnified SEM image (Figure 3c) presents the round-shaped morphology of deposited Pd crystals. The experimental set up was similar, as mentioned earlier for the decomposition of orange II dye. The complete removal of total organic carbon (TOC) was attained at 300 °C and 10 MPa pressure within a short residence time of 3.2 s. We also studied the effects of temperature, pressure, the initial concentration of the dye and residence time on catalytic activity, which is explained in detail in a following section of this paper, “factors affecting catalytic activity”.

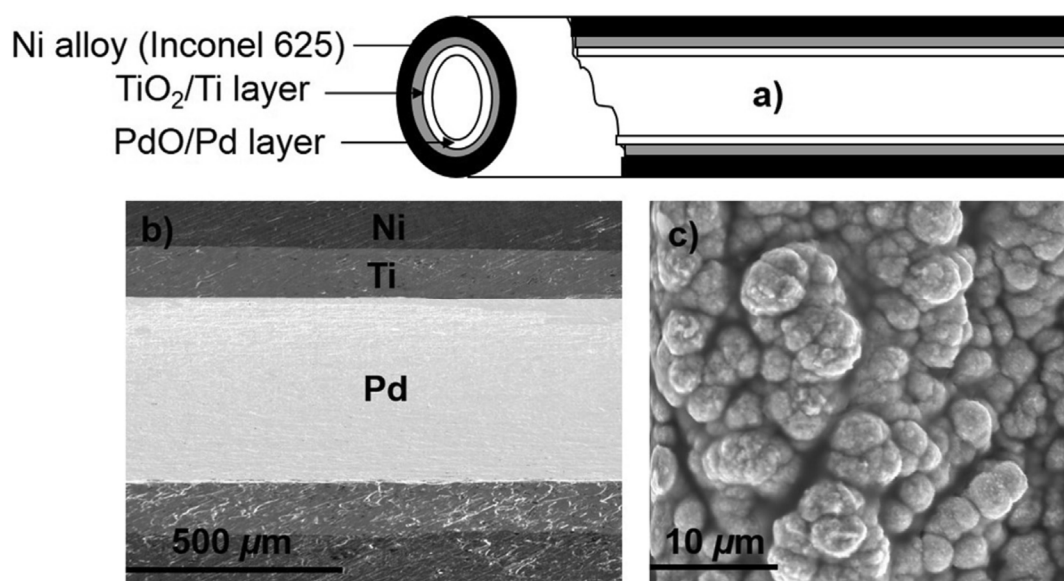


Figure 3. Images of the catalytic tubular reactor: (a) Schematic presentation of the tubular reactor; (b) Energy-dispersive X-ray spectroscopy (EDX) mapping of the longitudinal section of the Ni alloy (Inconel 625) tube with the TiO_2/Ti secondary layer coated with the thin Pd layer; (c) Scanning electron microscopy (SEM) image of deposited Pd [180].

A catalytic flow reaction system using a tubular reactor coated with a thin layer of PdO provided a continuous and efficient approach to the complete removal of synthetic dyes. In contrast to the packed-bed reactor, our hollow tubular reactor coated with a thin layer of metal catalyst provided a smooth and continuous flow of reaction medium. Moreover, no deactivation or leaching of metal catalyst was observed. The durability and robustness enabled repeated use of the catalytic tubular reactor. This approach of tubular reactors coated with a thin layer of catalyst using HPHT- H_2O provides an efficient technique for the complete removal of synthetic dyes within a very short residence time. Moreover, in contrast to other catalytic approaches, this process does not strictly depend on the pH of the reaction medium, which leads to the broad applicability of this technique.

6. Sulfate Radical-Based Catalytic Oxidation

Recently, the sulfate radical-based catalytic oxidation technique has attracted considerable attention for the decomposition of dyes in wastewaters. Sulfate radicals have been described as more efficient compared to hydroxyl radicals. For example, sulfate radicals possess a higher oxidation potential (2.5–3.1 V) [198–202] and react efficiently over a wide pH range (2–9) [198–201]. In addition, these radicals have a longer lifetime and react more selectively and efficiently by electron transfer with organic compounds containing unsaturated bonds or aromatic pi electrons [203–205].

In general, peroxymonosulfate (PMS) and persulfate (PS) are considered as oxidants to generate sulfate radicals [206]. The activation of PMS and PS is attained by various methods including heat, UV, ultrasound, or the use of a catalyst [201,206,207]. Several studies have reported the application of transition metal-based catalysts to activate PMS and PS. The catalytic activation of PS results in sulfate radicals, while that of PMS produces one hydroxyl and one sulfate radical [202]. In addition, PMS on reaction with the oxidized metal generates a sulfur pentoxide radical, which is less reactive than sulfate radicals but is capable of decomposing dye in wastewaters [202]. Figure 4, adapted from the published article [202], demonstrates the activation mechanism of PMS and PS by the catalyst.

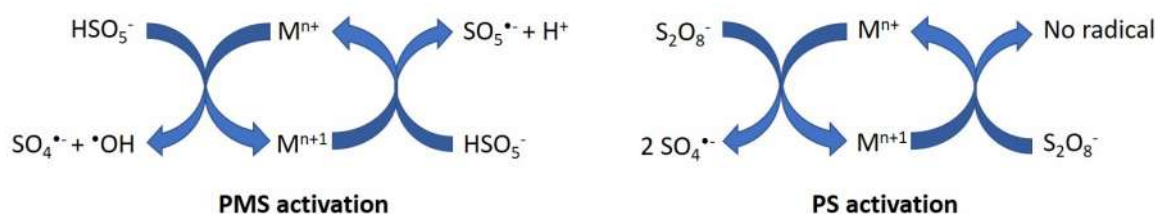


Figure 4. Transition metal-based catalytic activation of peroxymonosulfate (PMS) and persulfate (PS) [202].

Cobalt (Co) and silver (Ag) have proven to be the most effective transition metals for the activation of PMS and PS, respectively [201,202]. Mostly, the Co/PMS system has been studied for the removal of dyes. As homogeneous Co^{2+} /PMS leads to secondary water pollution [198,199,208], heterogeneous cobalt/PMS systems were also introduced. These heterogeneous catalysts included carbon [209], C_3N_4 [210] or metal oxide supported catalysts [211,212]. Heterogeneous catalysts provide the advantage of less or no metal contamination and show superior catalytic activity to degrade the harmful dyes dispersed in water bodies. Shukla et al. synthesized cobalt ion-exchanged zeolites using ZSM-5, zeolite-A, and zeolite-X as supports where the highly efficient degradation of phenol was attained by CO-ZSM-5 [169]. Wang et al. prepared an Al_2O_3 -based $CoFe_2O_4$ catalyst using a sol-gel method exhibiting high degradation efficiency of sulfachloropyridazine [213]. Hu et al. prepared nickel-foam supported Co_3O_4 - Bi_2O_3 catalysts for bisphenol A (BPA) removal by peroxymonosulfate activation at room temperature conditions [198]. Over 91% of BPA was degraded in a pH range of 3.0–7.0 within a reaction time of 30 min. In contrast to the hydroxyl radical system, sulfate radical-based catalytic oxidation has the potential to attain high activity within a broad pH range which increases the applicability of this approach to the degradation of a wide variety of pollutants in industrial effluents. In another paper by these authors [199], they applied $ZnCo_2O_4$ catalyst/PMS to BPA removal. They prepared catalysts changing different variables, including microwave temperature, microwave duration, calcination temperature, and calcination duration. Under the conditions of $[ZnCo_2O_4]$ as 0.2 gL^{-1} and $[PMS]/[BPA]_{\text{molar}}$ as 2.0, a BPA degradation efficiency of 99.28% was obtained within 5 min. Over 98.21% of BPA was degraded within a pH range of 4.0–9.0. In all the above mentioned published papers, researchers have emphasized the suitability of the sulfate radical-based catalytic technique for the treatment of wastewater at a wide range of pH.

7. Factors Affecting Catalytic Activity

7.1. pH

Generally, the quality of water is complex, and it exists at any pH value. Therefore, it is very important to determine the effect of the pH on the degradation efficiency of the catalytic system. Catalytic oxidation using H_2O_2 as an oxidant is influenced by the pH of the reaction medium [214]. The Fenton process is strongly dependent on the pH of the solution as it controls the production of hydroxyl radicals and the concentration of ferrous ions. An acidic medium is preferred for the decomposition of dyes using Fenton reagent [215,216]. The activity of Fenton reagent is reduced at higher pH due to

the formation of relatively inactive iron oxohydroxides and ferric hydroxide precipitates [214–216], while a reaction medium with a highly acidic pH is also considered inefficient [217]. The plausible cause of reduced activity at very low pH is associated with the existence of iron complex species $[\text{Fe}(\text{H}_2\text{O})_6]^{2+}$, which reacts more slowly with H_2O_2 than other species [218]. Another assumption is solvation of the peroxide in the presence of a high concentration of H^+ ions to form a stable oxonium ion $[\text{H}_3\text{O}_2]^+$. Oxonium ions make H_2O_2 more stable and reduce its reactivity with ferrous ions [217]. Therefore, the efficiency of the Fenton process is reduced both at high and very low pH. For Fenton-like oxidation using various metals in addition to Fe, the efficiency for dye degradation also reduces with the increasing alkalinity of the solution [99,218–220]. This decline in efficiency is attributed to the rapid conversion of hydroxyl radicals to its less active conjugate base, $\bullet\text{O}^-$ [221].

During our research on the catalytic decomposition of H_2O_2 using Pd or Pt-coated tubular reactors, we found that the catalytic conversion of H_2O_2 to hydroxyl radicals increased with increasing pH using oxidized Pd-coated tubular reactors at room temperature [191,222]. The optimized range of pH was described as 6–9. An increase in the acidity of the solution drastically decreased the decomposition of H_2O_2 . On the other hand, the Pt-coated tubular reactor did not show any significant decrease in the conversion of H_2O_2 to hydroxyl radicals on reducing the pH of the solution. The oxidized Pd surface was supposed to be more susceptible to proton and/or anion interaction, thereby the access of H_2O_2 molecules must be suppressed, leading to the inhibition in decomposition, whereas the easy access of H_2O_2 molecules to the Pt surface increased its catalytic efficiency [191,193]. Hence, the suitable pH range varies from metal to metal used as a catalyst for the decomposition of H_2O_2 .

A catalytic process using a sulfate radical as oxidant presents a system suitable for the dye decomposition at a broader range of pH than that using a hydroxyl radical [198–202]. However, a highly alkaline medium decreases the degradation efficiency. This phenomenon is suggested due to the excessive formation of OH^- , which generates hydroxyl radicals by consuming sulfate radicals. The weak oxidative ability and non-selectivity of hydroxyl radicals along with a decrease in the concentration of sulfate radicals decrease the efficiency for dye decomposition [202]. Therefore, it is required to optimize the pH of the reaction medium, which depends not only on the catalyst but is also highly influenced by the type of oxidant used in the process.

7.2. Temperature

It is reported in many research papers that an increase in operational temperature could be beneficial for both the oxidation rate and the extent of the catalytic decomposition of synthetic dyes [218,222], whereas very limited research has been conducted to evaluate the influence of experimental temperature conditions on the performance of the catalyst for the decomposition of synthetic dyes. Mostly, Fenton-based methods have been carried out at room temperature [223]. Zazo et al. [223] reported a considerable improvement in the decomposition of phenol (a primary component of most of the synthetic dyes) by Fenton oxidation at a relatively higher temperature, where a decomposition efficiency of almost 80% was achieved at 120 °C, which declined to 28% on decreasing the experimental temperature to 25 °C. The authors also demonstrated an enhanced iron-catalyzed H_2O_2 decomposition into radicals at a higher temperature. Salem et al., also investigated the effect of temperature on the decolorization efficiency of acid blue 29 dye using a heterogenous Cu catalyst, keeping the concentrations of the dye, H_2O_2 and the catalyst constant [176]. They noticed an increase in the decolorization efficiency from 51.8 to 88.2% on increasing the operating temperature from 20 to 40 °C within 18 min of reaction time.

The effect of temperature can also be associated with enhancing efficiency within a short residence time while keeping all other parameters fixed. During our research on the catalytic decomposition of synthetic dyes using a PdO-coated tubular reactor and HPHT- H_2O as reaction medium along with H_2O_2 as an oxidant, we observed that the reaction was strongly dependent on temperature [179,180]. While using a reaction solution of Orange II (a synthetic dye), COD removal of 84.0% was attained at 200 °C, which increased to 99.0% on increasing experimental temperature to 300 °C within a residence

time of 4 s and at a fix gauge pressure of 10 MPa [179]. Likewise, in another study on a solution of 20 ppm Remazol Brilliant Blue R dye, TOC removal enhanced sharply from 89 to 92 and 99.9% on increasing temperature from 200 to 250 and 300 °C, respectively, at 10 MPa pressure and a short residence time of 3.2 s [180]. Therefore, the catalytic decomposition of synthetic dyes at comparably higher temperatures provides a way to enhance the activity by a significant improvement of the oxidation rate and mineralization percentage within a fixed reaction time.

The catalytic process using a sulfate radical as an oxidant is also mostly studied at ambient temperature conditions [198–202] without considering the effect of operating temperature. Hence, the importance of temperature as a parameter in the catalytic decomposition of dyes cannot be denied. Therefore, a detailed investigation of the influence of temperature is highly required.

7.3. The Concentration of the Oxidant

The concentration of the oxidant plays a crucial role in the overall efficiency of the catalytic degradation process of dyes [126]. It is observed that the efficiency for the degradation of the synthetic dyes increased with an increase in the concentration of H₂O₂ in the reaction stream [224–227]. The steady-state concentration of hydroxyl radicals depends on the concentration of H₂O₂ and Fe²⁺ in the Fenton oxidation process. Tian et al., [228] reported that the color and COD removal increased to 94 and 50.7%, respectively, as the H₂O₂ increased to 125 mg/L in the Fenton process, while a further increase in the concentration of H₂O₂ decreased removal efficiency [228]. Similar results were also reported by other researchers [229]. The decrease in efficiency for dye decomposition on increasing H₂O₂ above the optimized concentration was attributed to the development of competition for adsorption on the surface of the catalyst, where the excessive H₂O₂ limits the access of the dye molecules. Besides, excessive H₂O₂ could reduce hydroxyl radicals as a radical scavenger [229,230]. Therefore, optimization of the H₂O₂ concentration in the catalytic oxidation process is highly important. As a study on iron-free catalytic oxidation, Salem, et al. examined the effect of H₂O₂ concentration on reaction rate for the decomposition of acid blue 29 dye using a Cu-based catalyst by maintaining the temperature, amount of catalyst and dye constant [223]. They reported an increase in decolorization efficiency from 26.6 to 84.3% on increasing H₂O₂ concentration from 0.02 to 0.4 M within 15 min. They attributed their findings to the enhanced generation of peroxo-intermediate or hydroxyl radicals on the increasing concentration of H₂O₂ in the reaction medium. The generation of peroxo-radicals in Cu-facilitated oxidation reactions were also reported by other researchers [231,232]. However, optimization for the required concentration of H₂O₂ should be conducted depending on the concentration of the synthetic dyes to be decomposed as the remaining concentration of unused H₂O₂ contributes to COD and is harmful to many of the organisms [226,227].

7.4. The Initial Concentration of Dye

The initial concentration of dye plays an important role in practical applications. In general, a lower initial concentration is favored [23,226,231] to attain the efficient and complete decomposition of the dyes. As the effluent released from industries contains a very high concentration of the dye contents, dilution is required before proceeding for catalytic treatment regardless of the type of oxidant used [23,176,226]. Salem et al., observed a significant decrease in the efficiency for dye decolorization from 92.8 to 78.2% on the increasing concentration of acid blue 29 dye from 1×10^{-4} to 2×10^{-5} M, while working with a heterogenous Cu catalyst and keeping the concentration of H₂O₂ constant (0.2 M) [223]. During the application of an oxidized Pd-coated tubular reactor to the decomposition of synthetic dyes using a fixed concentration of H₂O₂ as an oxidant at high temperature and pressure conditions, we observed that an increase in the initial concentration of synthetic dye decreased the efficiency for decomposition [179,180]. At higher dye concentrations, the generation of hydroxyl radicals on the surface of the catalyst was suggested to be reduced since the active sites of the catalyst might be occupied by the dye molecules. An increased number of dye molecules and insufficient concentration of the active radicals decreased the efficiency of

the decomposition process [176,179,180,224]. In contrast, Hassan et al. reported an increase in dye removal efficiency with increasing initial dye concentration [224,225]. This fact was associated with an increase in the probability of collision between the dye molecules and the oxidizing species on increasing the dye concentration in the reaction medium. However, the selection of the initial concentration of the dyes in reactants is also dependent on the concentration of the oxidizing agent, catalyst, and reaction/residence time of the process. For example, the initial concentration of synthetic dye is assessed by the amount of Fenton's reagent used in the process [227].

7.5. Reaction Time

Reaction/residence time is an important parameter influencing the catalytic dye decomposition process regardless of the type of catalyst (homogeneous or heterogeneous). Generally, the rate of the decomposition reaction increases with an increase in the duration or residence time of a reaction, while keeping all other factors, e.g., pH, temperature, concentrations of dye, oxidant and the catalyst constant. Soraya Mohajeri et al. reported the effect of reaction time on the Fenton process [233]. They varied the reaction time from 30 to 120 min and observed increased COD and color removal from 45 to 69%. S. Karthikeyan et al. also noticed a linear increase in the removal of COD within 4 h of the homogeneous Fenton oxidation reaction, which slowed down on increasing the reaction time for a further 2 h [234]. They attributed this initial linear increase in COD reduction to the chemical oxidation of the dissolved organics in wastewater with hydroxyl radicals. The authors also confirmed the higher efficiency of heterogeneous Fenton oxidation compared to the homogenous process. An overall COD removal of 90% of the textile wastewater was obtained for a heterogenous catalyst in approximately 4 h, whereas a COD removal of 50% was attained for the homogeneous catalyst within a reaction time of 6 h.

Usually, a long reaction time in hours is required to attain a significantly increased COD and color removal, whereas the decomposition of dyes with an efficiency above 99% of COD removal can be obtained within a few seconds using a thin metal catalyst-coated tubular reactor and HPHT-H₂O as the reaction medium [179,180]. The reaction time depends on other factors, including the temperature and concentration of the reacting species, etc. During our research on the catalytic decomposition of synthetic dyes using a PdO-coated tubular reactor, we observed that 89% TOC removal of Remazol Brilliant Blue R was obtained at 200 °C within a residence time of 3.9 s, which increased to 92 and 99.9 at 250 °C and 300 °C within a residence time of 3.6 and 3.2 s, respectively [180].

8. Conclusions

Dyes are one of the major pollutants of our environment. If these dyes are not removed from industrial effluents before entering into the aquatic system, this could be very harmful to all species on earth. The conventional methods are not very efficient in treating industrial wastewaters containing higher concentrations of synthetic dyes due to their recalcitrant nature and resistance to biodegradation. Catalytic oxidation is one of the advanced oxidation processes and is considered environmentally friendly and highly efficient for the degradation of dyes. The total mineralization of dyes is achieved in many processes. The Fenton reaction treatment is known to be very useful in the removal of dyes from wastewater using iron-based catalysts. Research efforts have also been focused on the establishment of iron-free catalytic systems using various other metals for the activation of H₂O₂. Tubular reactors with inner walls coated with a thin layer of metal catalysts have also been applied and found to be an efficient method for dye decomposition within a short residence time, i.e., seconds. Sulfate radical-based oxidation provides another efficient approach to the catalytic degradation of synthetic dyes.

The most challenging issue in the catalytic oxidation of synthetic dyes is the optimization of various reaction parameters as most catalytic processes depend heavily on various factors including pH, temperature, the concentration of the oxidant, the initial concentration of dyes and the reaction time. There exists an optimal value for almost every parameter depending on the type of catalyst and the oxidant to be used. By optimizing different factors appropriately, catalytic activity can

be enhanced to the greatest extent, making this one of the most advanced oxidation processes for dye degradation.

Funding: This research received no external funding.

Conflicts of Interest: The authors declare no conflict of interest.

References

1. Arena, F.; Chio, R.; Gumina, B.; Spadaro, L.; Trunfio, G. Recent advances on wet air oxidation catalysts for treatment of industrial wastewaters. *Inorg. Chimica Acta* **2015**, *431*, 101–109. [[CrossRef](#)]
2. Arena, F.; Italiano, C.; Ferrante, G.D.; Trunfio, G.; Spadaro, L. A mechanistic assessment of the wet air oxidation activity of MnCeOx catalyst toward toxic and refractory organic pollutants. *Appl. Catal. B Environ.* **2014**, *144*, 292–299. [[CrossRef](#)]
3. Arena, F.; Lombardo, D.; Ferrante, G.D.; Italiano, C.; Spadaro, L.; Trunfio, G. Highly effective oxide catalyst for the detoxification of oil wastewaters by the wet air oxidation process. *Desalin. Water Treatment* **2015**, *53*, 1018–1023. [[CrossRef](#)]
4. Arena, F.; Chio, R.; Gumina, B.; Spadaro, L.; Trunfio, G. Catalytic wet air oxidation (CWAO) of industrial wastewaters: Mechanistic evidences, catalyst development and kinetic modeling. In *Frontiers International Conference on Wastewater Treatment and Modelling*; Springer: Cham, Switzerland, 2017; Volume 4, pp. 349–353.
5. Shukla, S.P.; Mohan, D. Toxicity of disperse dyes and its removal from wastewater using various adsorbents: A review. *Res. J. Environ. Toxicol.* **2017**, *11*, 72–89.
6. Uday, U.S.P.; Bandyopadhyay, T.K.; Bhunia, B. Bioremediation and detoxification technology for treatment of dye(s) from textile effluent. In *Textile Wastewater Treatment*; IntechOpen: London, UK, 2016; pp. 75–92. ISBN 978-953-51-2543-3.
7. Allen, S.J.; McKay, G.; Porter, J.F. Adsorption isotherm models for basic dye adsorption by peat in single and binary component systems. *J. Colloid Interface Sci.* **2004**, *280*, 322–333. [[CrossRef](#)] [[PubMed](#)]
8. Bansal, P.; Sud, D. Photodegradation of commercial dye, CI reactive blue 160 using ZnO nanopowder: Degradation pathway and identification of intermediates by GC/MS. *Sep. Purif. Technol.* **2012**, *85*, 112–119. [[CrossRef](#)]
9. Champagne, P.; Nesheim, M.E.; Ramsay, J.A. Effect of a non-ionic surfactant, Merspol, on dye decolorization of reactive blue 19 by laccase. *Enzym. Microb. Technol.* **2010**, *46*, 147–152. [[CrossRef](#)]
10. Mansoorian, H.J.; Bazrafshan, E.; Yari, A.; Alizadeh, M. Removal of azo dyes from aqueous solution using Fenton and modified Fenton processes. *Health Scope* **2014**, *3*, e15507. [[CrossRef](#)]
11. Chander, R.; Naveen, S.; Arora, K.; Kothari, R. *Environmental Biotechnology: For Sustainable Future*; Springer: Singapore, 2019; ISBN 9789811072833.
12. Bharagava, R.N. *Emerging and Eco-Friendly Approaches for Waste Management*; Springer: Singapore, 2019; ISBN 9789811086687.
13. Jorge, A.; Rosa, M.; Garcia, V.S.G.; Boiani, F.; Melo, C.G.; Pereira, M.C.; Borrelly, S.I. Toxicity and environmental impacts approached in the dyeing of polyamide, polyester and cotton knits. *J. Environ. Chem. Eng.* **2019**, *7*, 102973.
14. Mahalingam, S.; Ramasamy, J. Enhanced photocatalytic degradation of synthetic dyes and industrial dye wastewater by hydrothermally synthesized G-CuO-Co₃O₄ hybrid nanocomposites under visible light irradiation. *J. Clust. Sci.* **2018**, *29*, 235–250. [[CrossRef](#)]
15. Ganzenko, O.; Trellu, C.; Papirio, S.; Oturan, N.; Huguenot, D.; Van Hullebusch, E.D.; Esposito, G.; Oturan, M.A. Bioelectro-Fenton: Evaluation of a combined biological-advanced oxidation treatment for pharmaceutical wastewater. *Environ. Sci. Pollut. Res.* **2017**, *25*, 20283–20292. [[CrossRef](#)] [[PubMed](#)]
16. Ganzenko, O.; Huguenot, D.; Van Hullebusch, E.D.; Esposito, G.; Oturan, M.A. Electrochemical advanced oxidation and biological processes for wastewater treatment: A review of the combined approaches. *Environ. Sci. Pollut. Res.* **2014**, *21*, 8493–8524. [[CrossRef](#)] [[PubMed](#)]
17. Madrakian, T.; Afkhami, A.; Ahmadi, M. Simple in-situ functionalizing magnetite nanoparticles by reactive blue-19 and their application to the effective removal of Pb²⁺ ions from water samples. *Chemosphere* **2013**, *90*, 542–547. [[CrossRef](#)] [[PubMed](#)]

18. Luo, Y.; Guo, W.; Hao, H.; Duc, L.; Ibney, F.; Zhang, J.; Liang, S.; Wang, X.C. A review on the occurrence of micropollutants in the aquatic environment and their fate and removal during wastewater treatment. *Sci. Total Environ.* **2014**, *473*, 619–641. [[CrossRef](#)] [[PubMed](#)]
19. da Silva, M.E.; Firmino, P.I.; dos Santos, A.B. Impact of the redox mediator sodium anthraquinone-2,6-disulphonate (AQDS) on the reductive decolourisation of the azo dye reactive red 2 (RR2) in one and two-stage anaerobic systems. *Bioresour. Technol.* **2012**, *121*, 1–7. [[CrossRef](#)]
20. Shah, P.D.; Dave, S.R.; Rao, M.S. Biodegradation enzymatic degradation of textile dye reactive orange 13 by newly isolated bacterial strain *alcaligenes faecalis* PMS-1. *Int. Biodeterior. Biodegrad.* **2012**, *69*, 41–50. [[CrossRef](#)]
21. De Oliveira, D.M.; Cavalcante, R.P.; De Melo, L.; Sans, C.; Esplugas, S. Identification of intermediates, acute toxicity removal, and kinetics investigation to the Ametryn treatment by direct photolysis (UV 254), UV 254/H₂O₂, Fenton, and photo-Fenton processes. *Environ. Sci. Pollut. Res.* **2019**, *26*, 4348–4366. [[CrossRef](#)]
22. Richardson, S.D.; Kimura, S.Y. Environmental contaminants: Challenges facing our next generation and potential engineering solutions. *Environ. Technol. Innov.* **2017**, *8*, 40–56. [[CrossRef](#)]
23. Babuponnusami, A.; Muthukumar, K. A review on Fenton and improvements to the Fenton process for wastewater treatment. *J. Environ. Chem. Eng.* **2013**, *2*, 557–572. [[CrossRef](#)]
24. Zhang, Y.; Zhang, N.; Wang, T.; Huang, H.; Chen, Y. Heterogeneous degradation of organic contaminants in the photo-Fenton reaction employing pure cubic β -Fe₂O₃. *Appl. Catal. B Environ.* **2019**, *245*, 410–419. [[CrossRef](#)]
25. Zhang, L.P.; Liu, Z.; Faraj, Y.; Zhao, Y.; Zhuang, R.; Xie, R.; Ju, X.; Wang, W.; Chu, L. High-flux efficient catalytic membranes incorporated with iron-based Fenton-like catalysts for degradation of organic pollutants. *J. Memb. Sci.* **2018**, *573*, 493–503. [[CrossRef](#)]
26. Lyu, L.; Han, M.; Cao, W.; Gao, Y.; Zeng, Q.; Yu, G.; Hunag, X.; Hu, C. Efficient Fenton-like process for organic pollutant degradation on Cu-doped mesoporous polyimide nanocomposites. *Environ. Sci. Nano* **2019**, *6*, 798–808. [[CrossRef](#)]
27. Sun, Y.; Yang, Z.; Tian, P.; Sheng, Y.; Xu, J.; Han, Y. Oxidative degradation of nitrobenzene by a Fenton-like reaction with Fe-Cu bimetallic catalysts. *Appl. Catal. B Environ.* **2018**, *244*, 1–10. [[CrossRef](#)]
28. Matavos-aramyan, S.; Moussavi, M. Advances in Fenton and Fenton based oxidation processes for industrial effluent contaminants control—A review. *Int. J. Environ. Sci. Nat. Resour.* **2017**, *2*, 1–18.
29. Miller, M.E. *Series in Display Science and Technology Color in Electronic Display Systems*; Springer: Switzerland, 2019; ISBN 9783030028336.
30. Moussavi, G.; Mahmoudi, M. Removal of azo and anthraquinone reactive dyes from industrial wastewaters using MgO nanoparticles. *J. Hazard. Mater.* **2009**, *168*, 806–812. [[CrossRef](#)]
31. Radi, M.A.; Mirjalili, N.N.M.; Moghadam, M.R. Ultrasound-assisted electrochemical decolorization of anthraquinone dye C.I reactive blue 49, its optimization and synergic effect: A comparative study. *Int. J. Environ. Sci. Technol.* **2019**, *16*, 2455–2464. [[CrossRef](#)]
32. Gurses, A.; Acikyildiz, M.; Gunes, K.; Gurses, M.S. *Dyes and pigments: Their structure and properties*; Springer: Cham, Switzerland, 2016; ISBN 9783319338903.
33. Oros, G.; Forgacs, E.; Cserha, T. Removal of synthetic dyes from wastewaters: A review. *Environ. Int.* **2004**, *30*, 953–971.
34. Nidheesh, P.V.; Gandhimathi, R. Trends in electro-Fenton process for water and wastewater treatment: An overview. *Desalination* **2012**, *299*, 1–15. [[CrossRef](#)]
35. Xu, H.; Sun, X.; Wang, S.; Song, C.; Wang, S. Development of laccase/graphene oxide membrane for enhanced. *Sep. Purif. Technol.* **2018**, *204*, 255–260. [[CrossRef](#)]
36. Kanagaraj, J.; Senthilvelan, T.; Panda, R.C. Degradation of azo dyes by laccase: Biological method to reduce pollution load in dye wastewater. *Clean Technol. Environ. Policy* **2015**, *17*, 1443–1456. [[CrossRef](#)]
37. Carmen, Z.; Daniela, S. Textile organic dyes; characteristics, polluting effects and separation/elimination procedures from industrial effluents; a critical overview. In *Organic Pollutants Ten Years after the Stockholm Convention-Environmental and Analytical Update*; IntechOpen: London, UK, 2012; ISBN 9789533079172.
38. Balapure, K.; Bhatt, N.; Madamwar, D. Mineralization of reactive azo dyes present in simulated textile waste water using down flow microaerophilic fixed film bioreactor. *Bioresour. Technol.* **2015**, *175*, 1–7. [[CrossRef](#)] [[PubMed](#)]

39. Ayaz, M.; Ayaz, M.; Ali, F.; Saeed, A.; Khurshid, A.; Shabir, G.; Ahmad, T.; Asad, S.; Kazmi, R.; Khan, H.A. Synthesis of symmetric bridged bis-pyrazolone based metal complex acid dyes and their applications on leather. *J. Fluoresc.* **2018**, *28*, 1181–1193. [[CrossRef](#)] [[PubMed](#)]
40. Kumar, S.; Raut, S.; Bandyopadhyay, P. Fungal decolouration and degradation of azo dyes: A review. *Fungal Biol. Rev.* **2016**, *30*, 112–133.
41. Solís, M.; Solís, A.; Inés, H.; Manjarrez, N.; Flores, M. Microbial decolouration of azo dyes: A review. *Process Biochem.* **2012**, *47*, 1723–1748. [[CrossRef](#)]
42. Sudha, M.; Saranya, A.; Selvakumar, G.; Sivakumar, N. Microbial degradation of Azo Dyes: A review. *Int. J. Curr. Microbiol. Appl. Sci.* **2014**, *3*, 670–690.
43. Delclos, K.B.; Tarpley, W.G.; Miller, E.C.; Miller, J.A. 4-aminoazobenzene and N,N-dimethyl-4-aminoazobenzene as equipotent hepatic carcinogens in male C57BL/6x C3H/He F₁ mice and characterization of A/(deoxyguanosin-8-yl)-4-aminoazobenzene as the major persistent hepatic DMA-bound dye in these mice. *Cancer Res.* **1984**, *44*, 2540–2550. [[PubMed](#)]
44. Cohen, S.M.; Boobis, A.R.; Dellarco, V.L.; Doe, J.E.; Fenner-Crisp, P.A.; Moretto, A.; Pastoor, T.P.; Schoeny, R.S.; Seed, J.G.; Wolf, D.C. Chemical carcinogenicity revisited 3: Risk assessment of carcinogenic potential based on the current state of knowledge of carcinogenesis in humans. *Regul. Toxicol. Pharmacol.* **2019**, *103*, 100–105. [[CrossRef](#)] [[PubMed](#)]
45. Chung, K.T. Azo dyes and human health: A review. *J. Environ. Sci. Health C Environ. Carcinog. Ecotoxicol. Rev.* **2016**, *34*, 233–261. [[CrossRef](#)] [[PubMed](#)]
46. Letters, C.; Sendai, H.C. Mutagenicity of metarolites of carcinogenic aminoazo dyes. *Cancer Lett.* **1979**, *8*, 71–76.
47. Thomas, N.S.; George, K.; Namasivayam, N. Molecular aspects and chemoprevention of dimethylaminoazobenzene-induced hepatocarcinogenesis: A review. *Hepatol. Res.* **2016**, *46*, 72–88. [[CrossRef](#)] [[PubMed](#)]
48. Li, W.; Chen, F.; Wang, S. Binding of reactive brilliant red to human serum albumin: Insights into the molecular toxicity of sulfonic azo dyes. *Protein Pept. Lett.* **2010**, *17*, 621–629. [[CrossRef](#)] [[PubMed](#)]
49. Wu, M.; Sun, L.; Miao, K.; Wu, Y.; Fan, L.J. Detection of sudan dyes based on inner filter effect with reusable conjugated polymer fibrous membranes. *ACS Appl. Mater. Interfaces* **2018**, *10*, 8287–8295. [[CrossRef](#)] [[PubMed](#)]
50. Kabir, S.; Rehman, A. Carcinogenic potential of arylamine N-acetyltransferase in Asian populations. *J. Cancer Res. Pract.* **2018**, *5*, 131–135. [[CrossRef](#)]
51. Yang, B.; Gao, Y.; Yan, D.; Xu, H.; Wang, J. Degradation characteristics of color index direct blue 15 dye using iron-carbon micro-electrolysis coupled with H₂O₂. *Int. J. Environ. Res. Public Health* **2018**, *15*, 1523. [[CrossRef](#)] [[PubMed](#)]
52. Thyssen, J.P.; White, J.M.L. Epidemiological data on consumer allergy to *p*-phenylenediamine. *Contact Dermat.* **2008**, *59*, 327–343. [[CrossRef](#)] [[PubMed](#)]
53. Balachandramohan, J.; Anandan, S.; Sivasankar, T. A simple approach for the sonochemical synthesis of Fe₃O₄-guargum nanocomposite and its catalytic reduction of *p*-nitroaniline. *Ultrason. Sonochemistry* **2018**, *40*, 1–10. [[CrossRef](#)] [[PubMed](#)]
54. Mansour, H.B.; Aayed-ajmi, Y.; Mosrati, R.; Corroler, D.; Ghedira, K.; Barillier, D.; Chekir-ghedira, L. Acid violet 7 and its biodegradation products induce chromosome aberrations, lipid peroxidation, and cholinesterase inhibition in mouse bone marrow. *Environ. Sci. Pollut. Res.* **2010**, *17*, 1371–1378. [[CrossRef](#)]
55. Carreon, T.; Hein, M.J.; Viet, S.M.; Hanley, K.W.; Ruder, A.M.; Ward, E.M. Increased bladder cancer risk among workers exposed to o-toluidine and aniline: A reanalysis. *Occup. Environ. Med.* **2010**, *67*, 348–351. [[CrossRef](#)]
56. Morton, L.D.; Youssef, A.F.; Lloyd, E.; Kiorpes, A.L.; Goldsworthy, T.L.; Fort, F.L. Safety evaluation; food & chemical evaluation of carcinogenic responses in the Eker rat following short-term exposure to selected nephrotoxins and carcinogens. *Toxicol. Pathology* **2002**, *30*, 559–564.
57. Srivastava, S.; Sinha, R.; Roy, D. Toxicological effects of malachite green. *Aquat. Toxicol.* **2004**, *66*, 319–329. [[CrossRef](#)]
58. National Toxicology Program. Bioassay of 2-Nitro-*p*-phenylenediamine for Possible Carcinogenicity. *Natl. Cancer Inst. Carcinog. Tech. Rep. Ser.* **1979**, *169*, 1.
59. Brüscheweiler, B.J.; Merlot, C. Azo dyes in clothing textiles can be cleaved into a series of mutagenic aromatic amines which are not regulated yet. *Regul. Toxicol. Pharmacol.* **2017**, *88*, 214–226. [[CrossRef](#)] [[PubMed](#)]

60. Shao, Y.; Hollert, H.; Tarcai, Z.; Deutschmann, B.; Seiler, T. Science of the total environment integrating bioassays, chemical analysis and in silico techniques to identify genotoxicants in surface water. *Sci. Total Environ.* **2019**, *650*, 3084–3092. [[CrossRef](#)] [[PubMed](#)]
61. Singh, S.N. *Microbial Degradation of Synthetic Dyes in Wastewaters*; Springer: Switzerland, 2016; ISBN 9783319109411.
62. Dasgupta, N.; Lichtfouse, E. *Nanoscience and Biotechnology for Environmental Applications*; Springer: Switzerland, 2019; ISBN 9783319979212.
63. Deliyanni, E.A. Activated carbon supported MnO₂ for catalytic degradation of reactive black. *Colloids Surf. A* **2019**, *566*, 166–175.
64. Naseem, K.; Begum, R.; Farooqi, Z.H. Catalytic reduction of 2-nitroaniline: A review. *Environ. Sci. Pollut. Res.* **2017**, *24*, 6446–6460. [[CrossRef](#)] [[PubMed](#)]
65. Mahmood, S.; Khalid, A.; Arshad, M.; Mahmood, T.; Crowley, D.E. Detoxification of azo dyes by bacterial oxidoreductase enzymes. *Crit. Rev. Biotechnol.* **2016**, *36*, 639–651. [[CrossRef](#)] [[PubMed](#)]
66. Maria, F.; Chequer, D.; Mescoloto, T.; De Felício, R.; Valnice, M.; Zaroni, B.; Maria, H.; Peporine, N.; Palma, D.; Oliveira, D. Toxicology in vitro; the azo dye disperse red 13 and its oxidation and reduction products showed mutagenic potential. *Toxicol. Vitro.* **2015**, *29*, 1906–1915.
67. Muthu, S.S. Textile science and clothing technology. In *Detox Fashion*; Springer: Hong Kong, China, 2018; ISBN 9789811047794.
68. Watanabe, T.; Hirayama, T.; Fukui, S. The mutagenic modulating effect of *p*-phenylenediamine on the oxidation of *o*- or *m*-phenylenediamine with hydrogen peroxide in the Salmonella test. *Mutat. Res. Lett.* **1990**, *245*, 15–22. [[CrossRef](#)]
69. Shetti, N.P.; Malode, S.J.; Malladi, R.S.; Nargund, S.L.; Shukla, S.S.; Aminabhavi, T.M. Electrochemical detection and degradation of textile dye Congo red at graphene oxide modified electrode. *Microchem. J.* **2019**, *146*, 387–392. [[CrossRef](#)]
70. Chung, K.; Kirkovsky, L.; Kirkovsky, A.; Purcell, W.P. Review of mutagenicity of monocyclic aromatic amines: Quantitative structure—Activity relationships. *Mutat. Res./Rev. Mutat. Res.* **1997**, *387*, 1–16. [[CrossRef](#)]
71. Fenton, H.J.H. Oxidation of tartaric acid in presence of iron. *J. Chem. Soc. Trans.* **1894**, *65*, 899–910. [[CrossRef](#)]
72. Zhang, Y.; Zhou, M. A critical review of the application of chelating agents to enable Fenton and Fenton-like reactions at high pH values. *J. Hazard. Mater.* **2018**, *362*, 436–450. [[CrossRef](#)] [[PubMed](#)]
73. Mirzaei, A.; Chen, Z.; Haghghat, F.; Yerushalmi, L. Removal of pharmaceuticals from water by homo/heterogenous Fenton-type processes—A review. *Chemosphere* **2017**, *174*, 665–688. [[CrossRef](#)] [[PubMed](#)]
74. Pignatello, J.J.; Oliveros, E.; Mackay, A. Advanced oxidation processes for organic contaminant destruction based on the Fenton reaction and related chemistry. *Critical Rev. Environ. Sci. Technol.* **2006**, *36*, 1–84. [[CrossRef](#)]
75. Haber, F.; Weiss, J. The Catalytic decomposition of hydrogen peroxide by iron salts. *Proc. R. Soc. Lond. A* **1934**, *147*, 332–351.
76. Dewil, R.; Mantzavinos, D.; Poulios, I.; Rodrigo, M.A. New perspectives for advanced oxidation processes. *J. Environ. Manag.* **2017**, *195*, 93–99. [[CrossRef](#)] [[PubMed](#)]
77. Glaze, W.H.; Kang, J.; Douglas, H. Ozone: Science & engineering: The chemistry of water treatment processes involving ozone, hydrogen peroxide and ultraviolet radiation. *J. Int. Ozone Assoc.* **1987**, *9*, 335–352.
78. Hoigne, J. Inter-calibration of OH radical sources and water quality. *Water Sci. Technol.* **1997**, *35*, 1–8. [[CrossRef](#)]
79. Lloyd, R.V.; Hanna, P.M.; Mason, R.P. The origin of the hydroxyl radical oxygen in the Fenton reaction. *Free Radic. Biol. Med.* **1997**, *22*, 885–888. [[CrossRef](#)]
80. Yoon, J.; Lee, Y.; Kim, S. Investigation of the reaction pathway of OH radicals produced by Fenton oxidation in the conditions of wastewater treatment. *Water Sci. Technol.* **2001**, *44*, 15–22. [[CrossRef](#)]
81. Rigg, T.; Taylor, W.; Weiss, J. The rate constant of the reaction between hydrogen peroxide and ferrous ions. *J. Chem. Phys.* **1954**, *22*, 575–577. [[CrossRef](#)]
82. Jones, A.B.; Walling, C. Mechanism of the ferric ion catalyzed decomposition of hydrogen peroxide. effect of organic substrates. *J. Am. Chem. Soc.* **1973**, *591*, 2987–2991.
83. Bielski, B.H.J.; Cabelli, D.E.; Arudi, R.L.; Ross, A.B. Reactivity of HO₂/O₂ Radicals in Aqueous Solution. *J. Phys. Chem. Ref. Data* **1985**, *14*, 1041–1100. [[CrossRef](#)]

84. Buxton, G.V.; Greenstock, C.L.; Helman, W.P.; Ross, A.B.; Buxton, G.V.; Greenstock, C.L.; Helman, P.; Ross, A.B. Critical Review of rate constants for reactions of hydrated electrons, hydrogen atoms and hydroxyl radicals (OH/O in Aqueous Solution). *J. Phys. Chem. Ref. Data* **1988**, *17*, 513–886. [[CrossRef](#)]
85. Walling, C. Fenton's reagent revisited. *Acc. Chem. Res.* **1975**, *8*, 125–131. [[CrossRef](#)]
86. Arnold, S.M.; Hickey, W.J.; Harris, R.F. Degradation of Atrazine by Fenton's Reagent: Condition Optimization and Product. *Environ. Sci. Technol.* **1995**, *29*, 2083–2089. [[CrossRef](#)] [[PubMed](#)]
87. Tamimi, M.; Qourzal, S.; Barka, N.; Assabbane, A. Methomyl degradation in aqueous solutions by Fenton's reagent and the photo-Fenton system. *Sep. Purif. Technol.* **2008**, *61*, 103–108. [[CrossRef](#)]
88. Zhao, C.; Arroyo-mora, L.E.; Decaprio, A.P.; Sharma, V.K.; Dionysiou, D.D.; Shea, K.E.O. Reductive and oxidative degradation of iopamidol, iodinated X-ray contrast media, by Fe (III)-oxalate under UV and visible light treatment. *Water Res.* **2014**, *67*, 144–153. [[CrossRef](#)]
89. De Luna, L.A.V.; Thiago, H.G.; Pupo, R.F.; Kummrow, F.; Umbuzeiro, G.A. Aquatic toxicity of dyes before and after photo-Fenton treatment. *J. Hazard. Mater.* **2014**, *276*, 332–338. [[CrossRef](#)]
90. Voelker, B.M. Rates of hydroxyl radical generation and organic compound oxidation in mineral-catalyzed Fenton-like systems. *Environ. Sci. Technol.* **2003**, *37*, 1150–1158.
91. Hu, J.; Zhang, P.; An, W.; Liu, L.; Liang, Y.; Cui, W. In-situ Fe-doped g-C₃N₄ heterogeneous catalyst via photocatalysis-Fenton reaction with enriched photocatalytic performance for removal of complex wastewater. *Appl. Catal. B Environ.* **2019**, *245*, 130–142. [[CrossRef](#)]
92. Hammouda, S.B.; Salazar, C.; Zhao, F.; Ramasamy, D.L.; Laklova, E.; If tekhar, S.; Babu, I.; Sillanpää, M. Efficient heterogeneous electro-Fenton incineration of a contaminant of emergent concern-cotinine- in aqueous medium using the magnetic double perovskite oxide Sr₂FeCuO₆ as a highly stable catalyst: Degradation kinetics and oxidation products. *Appl. Catal. B Environ.* **2018**, *240*, 201–214. [[CrossRef](#)]
93. Meijide, J.; Pazos, M.; Sanromán, M.Á. Heterogeneous electro-Fenton catalyst for 1-butylpyridinium chloride degradation. *Environ. Sci. Pollut. Res.* **2019**, *26*, 3145–3156. [[CrossRef](#)] [[PubMed](#)]
94. Zárata-Guzmán, A.I.; González-Gutiérrez, L.V.; Godínez, L.A.; Carrasco-Marín, F.; Romero-Cano, L.A. Towards understanding of heterogeneous Fenton reaction using carbon-Fe catalysts coupled to in-situ H₂O₂ electro-generation as clean technology for wastewater treatment. *Chemosphere* **2019**, *224*, 698–706. [[CrossRef](#)] [[PubMed](#)]
95. Wang, Y.; Xi, Y.; Tian, H.; Fang, J.; Quan, X.; Pei, Y. Effects of reaction conditions and liquid property on degradation of phenol by RGO/ α -FeOOH supported on Al-MCM catalyst in heterogeneous photo-Fenton system. *Catal. Today* **2019**, in press. [[CrossRef](#)]
96. Zhang, C.; Ren, G.; Wang, W.; Yu, X.; Yu, F.; Zhang, Q.; Zhou, M. A new type of continuous-flow heterogeneous electro-Fenton reactor for tartrazine degradation. *Sep. Purif. Technol.* **2018**, *208*, 76–82. [[CrossRef](#)]
97. Zhou, M.; Oturan, M.A.; Sires, I. *Electro-Fenton Process, New Trends and Scale Up*; Springer: Singapore, 2018; ISBN 9789811064050.
98. Qiu, B.; Deng, Y.; Du, M.; Xing, M.; Zhang, J. Ultradispersed Cobalt Ferrite Nanoparticles Assembled in Graphene Aerogel for Continuous Photo-Fenton Reaction and Enhanced Lithium Storage Performance. *Sci. Rep.* **2016**, *6*, 29099. [[CrossRef](#)]
99. Oladipo, A.A.; If ebajo, A.O.; Gazi, M. Magnetic LDH-based CoO–NiFe₂O₄ catalyst with enhanced performance and recyclability for efficient decolorization of azo dye via Fenton-like reactions. *Appl. Catal. B Environ.* **2018**, *243*, 243–252. [[CrossRef](#)]
100. Yu, X.; Lin, X.; Feng, W.; Li, W. Enhanced catalytic performance of a bio-templated TiO₂ UV-Fenton system on the degradation of tetracycline. *Appl. Surf. Sci.* **2019**, *465*, 223–231. [[CrossRef](#)]
101. Soon, A.N.; Hameed, B.H. General degradation of acid blue 29 in visible light radiation using iron modified mesoporous silica as heterogeneous Photo-Fenton catalyst. *Appl. Catal. A Gen.* **2013**, *450*, 96–105. [[CrossRef](#)]
102. Gonzalez-Olmos, R.; Martin, M.J.; Georgi, A.; Kopinke, F.; Oller, I. Applied Catalysis B: Environmental Fe-zeolites as heterogeneous catalysts in solar Fenton-like reactions at neutral pH. *Appl. Catal. B Environ.* **2012**, *125*, 51–58. [[CrossRef](#)]
103. Yang, W.; Zhou, M.; Oturan, N.; Li, Y.; Su, P.; Oturan, M.A. Enhanced activation of hydrogen peroxide using nitrogen doped graphene for effective removal of herbicide 2,4-D from water by iron-free electrochemical advanced oxidation. *Electrochim. Acta* **2018**, *297*, 582–592. [[CrossRef](#)]
104. Mart, F.; Pariente, M.I.; Angel, J. Influence of preoxidizing treatments on the preparation of iron-containing activated carbons for catalytic wet peroxide oxidation of phenol. *J. Chem. Technol. Biotechnol.* **2012**, *87*, 880–886.

105. Grisales, C.M.; Salazar, L.M.; Garcia, D.P. Treatment of synthetic dye baths by Fenton processes: Evaluation of their environmental footprint through life cycle assessment. *Environ. Sci. Pollut. R.* **2019**, *26*, 4300–4311. [[CrossRef](#)] [[PubMed](#)]
106. Tarkwa, J.B.; Oturan, N.; Acayanka, E.; Laminsi, S.; Oturan, M.A. Photo-Fenton oxidation of Orange G azo dye: Process optimization and mineralization mechanism. *Environ. Chem. Lett.* **2018**, *17*, 473–479. [[CrossRef](#)]
107. Goi, A.; Trapido, M. Hydrogen peroxide photolysis, Fenton reagent and photo-Fenton for the degradation of nitrophenols: A comparative study. *Chemosphere* **2002**, *46*, 913–922. [[CrossRef](#)]
108. Ameta, R.; Chohadia, A.K.; Jain, A.; Punjabi, P.B. *Advanced Oxidation Processes for Wastewater Treatment: Fenton and Photo-Fenton Processes*; Elsevier: Amsterdam, The Netherlands, 2018; pp. 49–87. ISBN 9780128104996.
109. Shima, Q.; Pouran, R.; Aziz, A.R.A.; Mohd, W.; Wan, A. Review on the advances in photo-Fenton oxidation system for recalcitrant wastewaters. *J. Ind. Eng. Chem.* **2014**, *21*, 53–69.
110. Malato, S.; Maldonado, M.I.; Fernández-Ibáñez, P.; Oller, I.; Polo, I.; Sánchez-Moreno, R. Decontamination and disinfection of water by solar photocatalysis: The pilot plants of the Plataforma solar de Almeria. *Mater. Sci. Semicond. Process.* **2015**, *42*, 15–23. [[CrossRef](#)]
111. Spuhler, D.; Andre, J. The effect of Fe^{2+} , Fe^{3+} , H_2O_2 and the photo-Fenton reagent at near neutral pH on the solar disinfection (SODIS) at low temperatures of water containing Escherichia coli K12. *Appl. Catal. B Environ.* **2010**, *96*, 126–141. [[CrossRef](#)]
112. Faust, B.C.; Hoigne, J. Photolysis of Fe(III)-hydroxy complexes as sources of OH radicals in clouds, fog and rain. *Atmos. Environ. Part A Gen. Top.* **1990**, *24*, 79–89. [[CrossRef](#)]
113. Marinas, A.; Marinas, J.M.; Urbano, F.J. Comparative study of photocatalytic degradation of 3-chloropyridine under UV and solar light by homogeneous (photo-Fenton) and heterogeneous (TiO_2) photocatalysis. *Appl. Catal. B Environ.* **2012**, *127*, 316–322.
114. Hermosilla, D.; Cortijo, M.; Pao, C. Optimizing the treatment of land fill leachate by conventional Fenton and photo-Fenton processes. *Sci. Total Environ.* **2009**, *407*, 3473–3481. [[CrossRef](#)] [[PubMed](#)]
115. Yadav, M.; Gupta, R.; Sharma, R.K. *Green and Sustainable Pathways for Wastewater Purification*; Elsevier Inc.: Amsterdam, The Netherlands, 2019; ISBN 9780128147900.
116. Ribeiro, A.R.; Nunes, O.C.; Pereira, M.F.R.; Silva, A.M.T. An overview on the advanced oxidation processes applied for the treatment of water pollutants defined in the recently launched Directive 2013/39/EU. *Environ. Int.* **2015**, *75*, 33–51. [[CrossRef](#)] [[PubMed](#)]
117. Reyes, L.H. Determination of optimum operating parameters for Acid Yellow 36 decolorization by electro-Fenton process using BDD cathode. *Chem. Eng. J.* **2010**, *160*, 199–206.
118. Iurascu, B.; Siminiceanu, I.; Vione, D.; Vicente, M.A.; Gil, A.; Giuria, V.P.; Torino, I.; Analitica, C. Phenol degradation in water through a heterogeneous photo-Fenton process catalyzed by Fe-treated laponite. *Water Res.* **2009**, *43*, 1313–1322. [[CrossRef](#)] [[PubMed](#)]
119. Jo, W.; Tayade, R.J. New generation energy-efficient light source for photocatalysis: LEDs for environmental applications. *Ind. Eng. Chem. Res.* **2014**, *53*, 2073–2084. [[CrossRef](#)]
120. Pliego, G.; Xekoukoulotakis, N.; Venieri, D.; Zazo, J.A.; Casas, J.A.; Rodriguez, J.; Mantzavinos, D. Complete degradation of the persistent anti-depressant sertraline in aqueous solution by solar photo-Fenton oxidation. *J. Chem. Technol. Biotechnol.* **2014**, *89*, 814–818. [[CrossRef](#)]
121. Zhang, X.; Ma, J.; Fan, C.; Peng, M.; Komarneni, S. Enhancement of photo-fenton-like degradation of orange II by MnO_2/NiO nanocomposite with the synergistic effect from bisulfite. *J. Alloys Compd.* **2019**, *785*, 343–349. [[CrossRef](#)]
122. Kuo, W.S.; Wu, L.N. Fenton degradation of 4-chlorophenol contaminated water promoted by solar irradiation. *Sol. Energy* **2010**, *84*, 59–65. [[CrossRef](#)]
123. Jiang, Z.; Wang, L.; Lei, J.; Liu, Y.; Zhang, J. Photo-Fenton degradation of phenol by CdS/rGO/Fe^{2+} at natural pH with in-situ-generated H_2O_2 . *Appl. Catal. B Environ.* **2019**, *241*, 367–374. [[CrossRef](#)]
124. Karthikeyan, S.; Boopathy, R.; Gupta, V.K.; Sekaran, G. Preparation, characterizations and its application of heterogeneous Fenton catalyst for the treatment of synthetic phenol solution. *J. Mol. Liq.* **2013**, *177*, 402–408. [[CrossRef](#)]
125. Lagori, G.; Rocca, J.P.; Brulat, N.; Merigo, E.; Vescovi, P. Comparison of two different laser wavelengths' dental bleaching results by photo-Fenton reaction: In vitro study. *Laser Med. Sci.* **2015**, *30*, 1001–1006. [[CrossRef](#)] [[PubMed](#)]

126. Cruz, N.D.; Esplugas, S.; Grandjean, D.; Alencastro, L.F.; Pulgarin, C. Degradation of 32 emergent contaminants by UV and neutral photo-fenton in domestic wastewater effluent previously treated by activated sludge. *Water Res.* **2012**, *6*, 1947–1957. [[CrossRef](#)] [[PubMed](#)]
127. Guimarães, J.R.; Maniero, M.G.; De Araújo, R.N. A comparative study on the degradation of RB-19 dye in an aqueous medium by advanced oxidation processes. *J. Environ. Manag.* **2012**, *110*, 33–39. [[CrossRef](#)] [[PubMed](#)]
128. Abdul, M.; Khan, N.; Siddique, M.; Wahid, F.; Khan, R. Removal of reactive blue 19 dye by sono, photo and sonophotocatalytic oxidation using visible light. *Ultrason. Sonochemistry* **2015**, *26*, 370–377.
129. Silva, L.G.M.; Moreira, F.C.; Souza, A.A.U.; Souza, S.M.A.G.U.; Boaventura, R.A.R.; Vilar, V.J.P. Chemical and electrochemical advanced oxidation processes as a polishing step for textile wastewater treatment: A study regarding the discharge into the environment and the reuse in the textile industry. *J. Clean. Prod.* **2018**, *198*, 430–442. [[CrossRef](#)]
130. Sirés, I.; Brillas, E.; Oturan, M.A.; Rodrigo, M.A.; Panizza, M. Electrochemical advanced oxidation processes: Today and tomorrow. A review. *Environ. Sci. Pollut. Res.* **2014**, *21*, 8336–8367. [[CrossRef](#)]
131. He, H.; Zhou, Z. Electro-Fenton process for water and wastewater treatment. *Crit. Rev. Environ. Sci. Technol.* **2017**, *47*, 2100–2131. [[CrossRef](#)]
132. Nidheesh, P.V.; Gandhimathi, R. Degradation of dyes from aqueous solution by Fenton processes: A review. *Environ. Sci. Pollut. Res.* **2013**, *20*, 2099–2132. [[CrossRef](#)]
133. Kim, D.; Lee, D.; Monllor-satoca, D.; Kim, K.; Lee, W. Homogeneous photocatalytic Fe³⁺/Fe²⁺ redox cycle for simultaneous Cr(VI) reduction and organic pollutant oxidation: Roles of hydroxyl radical and degradation intermediates. *J. Hazard. Mater.* **2018**, in press. [[CrossRef](#)]
134. Sires, I.; Garrido, J.A.; Rodríguez, R.M.; Brillas, E.; Oturan, N.; Oturan, M.A.; Mar, R. Catalytic behavior of the Fe³⁺/Fe²⁺ system in the electro-Fenton degradation of the antimicrobial chlorophene. *Appl. Catal. B Environ.* **2007**, *72*, 382–394. [[CrossRef](#)]
135. Hammami, S.; Oturan, N.; Bellakhal, N.; Dachraoui, M.; Oturan, M.A. Oxidative degradation of direct orange 61 by electro-Fenton process using a carbon felt electrode: Application of the experimental design methodology. *J. Electroanal. Chem.* **2007**, *610*, 75–84. [[CrossRef](#)]
136. Wang, A.; Qu, J.; Ru, J.; Liu, H.; Ge, J. Mineralization of an azo dye Acid Red 14 by electro-Fenton's reagent using an activated carbon fiber cathode. *Dyes Pigments* **2005**, *65*, 227–233. [[CrossRef](#)]
137. Ali, O.; Şahin, Y.; Koparal, A.S.; Oturan, M.A. Carbon sponge as a new cathode material for the electro-Fenton process: Comparison with carbon felt cathode and application to degradation of synthetic dye basic blue 3 in aqueous medium. *J. Electroanal. Chem.* **2008**, *616*, 71–78.
138. Labiadh, L.; Oturan, M.A.; Panizza, M.; Ben, N.; Ammar, S. Complete removal of AHPS synthetic dye from water using new electro-fenton oxidation catalyzed by natural pyrite as heterogeneous catalyst. *J. Hazard. Mater.* **2015**, *297*, 34–41. [[CrossRef](#)] [[PubMed](#)]
139. Panizza, M.; Cerisola, G. Electro-Fenton degradation of synthetic dyes. *Water Res.* **2009**, *43*, 339–344. [[CrossRef](#)] [[PubMed](#)]
140. Meas-vong, Y.; Rodri, F.J.; Chapman, T.W.; Maldonado, M.I.; God, L.A. In-situ electrochemical and photo-electrochemical generation of the fenton reagent: A potentially important new water treatment technology. *Water Res.* **2006**, *40*, 1754–1762.
141. Zhang, H.; Fei, C.; Zhang, D.; Tang, F. Degradation of 4-nitrophenol in aqueous medium by electro-Fenton method. *J. Hazard. Mater.* **2007**, *145*, 227–232. [[CrossRef](#)]
142. Yu, F.; Zhou, M.; Zhou, L.; Peng, R. A novel electro-Fenton process with H₂O₂ generation in a rotating disk reactor for organic pollutant degradation. *Environ. Sci. Technol. Lett.* **2014**, *1*, 320–324. [[CrossRef](#)]
143. Nurhayati, E.; Yang, H.; Chen, C.; Liu, C.; Juang, Y. Electro-photocatalytic Fenton decolorization of orange G using mesoporous TiO₂/stainless steel mesh photo-electrode prepared by the sol-gel dip-coating method. *Int. J. Electrochem. Sci.* **2016**, *11*, 3615–3632. [[CrossRef](#)]
144. Liu, W.; Ai, Z.; Zhang, L. Design of a neutral three-dimensional electro-Fenton system with foam nickel as particle electrodes for wastewater treatment. *J. Hazard. Mater.* **2012**, *243*, 257–264. [[CrossRef](#)] [[PubMed](#)]
145. Rosales, E.; Iglesias, O.; Pazos, M.; Sanromán, M.A. Decolourisation of dyes under electro-Fenton process using Fe alginate gel beads. *J. Hazard. Mater.* **2012**, *213–214*, 369–377. [[CrossRef](#)] [[PubMed](#)]
146. Bocos, E.; Pazos, M.; Sanromán, M.A. Electro-Fenton decolourization of dyes in batch mode by the use of catalytic activity of iron loaded hydrogels. *J. Chem. Technol. Biotechnol.* **2014**, *89*, 1235–1242. [[CrossRef](#)]

147. Rostamizadeh, M.; Jafarizad, A.; Gharibian, S. High efficient decolorization of reactive red 120 azo dye over reusable Fe-ZSM-5 nanocatalyst in electro-Fenton reaction. *Sep. Purif. Technol.* **2017**, *192*, 340–347. [[CrossRef](#)]
148. Qiao, N.; Chang, J.; Hu, M.; Ma, H. Novel bentonite particle electrodes based on Fenton catalyst and its application in orange II removal. *Desalin. Water Treat.* **2016**, *57*, 17030–17038. [[CrossRef](#)]
149. Gogate, P.R. Treatment of wastewater streams containing phenolic compounds using hybrid techniques based on cavitation: A review of the current status and the way forward. *Ultrason. Sonochemistry* **2008**, *15*, 1–15. [[CrossRef](#)] [[PubMed](#)]
150. Adewuyi, Y.G. Perovskite-like catalysts LaBO₃ (B=Cu, Fe, Mn, Co, Ni) for wet peroxide oxidation of phenol. *Appl. Catal. B Environ.* **2001**, *180*, 4681–4715.
151. Kerabchi, N.; Merouani, S.; Hamdaoui, O. Relationship between liquid depth and the acoustic generation of hydrogen: Design aspect for large cavitation reactors with special focus on the role of the wave attenuation. *Int. J. Green Energy* **2019**, *16*, 1–12. [[CrossRef](#)]
152. Zhang, J.H.; Zou, H.Y.; Ning, X.A.; Lin, M.Q.; Chen, C.M.; An, T.C.; Sun, J. Combined ultrasound with Fenton treatment for the degradation of carcinogenic polycyclic aromatic hydrocarbons in textile dying sludge. *Environ. Geochem. Health* **2018**, *40*, 1867–1876. [[CrossRef](#)]
153. Liang, J.; Komarov, S.; Hayashi, N.; Kasai, E. Recent trends in the decomposition of chlorinated aromatic hydrocarbons by ultrasound irradiation and Fenton's reagent. *J. Mater. Cycles Waste Manag.* **2007**, *9*, 47–55. [[CrossRef](#)]
154. Wu, Z.; Yuste-córdoba, F.J.; Cintas, P.; Wu, Z.; Bo, L. Effects of ultrasonic and hydrodynamic cavitation on the treatment of cork wastewater by flocculation and Fenton processes. *Ultrason. Sonochemistry* **2017**, *40*, 3–8. [[CrossRef](#)] [[PubMed](#)]
155. Saleh, R.; Tau, A. Degradation of methylene blue and congo-red dyes using Fenton, photo-Fenton, sono-Fenton, and sonophoto-Fenton methods in the presence of iron (II, III) oxide/zinc oxide/graphene (Fe₃O₄/ZnO/graphene) composites. *Separ. Purif. Technol.* **2019**, *210*, 563–573. [[CrossRef](#)]
156. Khataee, A.; Rad, T.S.; Vahid, B.; Khorram, S. Preparation of zeolite nanorods by corona discharge plasma for degradation of phenazopyridine by heterogeneous sono-Fenton-like process. *Ultrason. Sonochemistry* **2016**, *33*, 37–46. [[CrossRef](#)] [[PubMed](#)]
157. Zou, H.; Ning, X.; Wang, Y.; Sun, J.; Hong, Y. Sono-advanced Fenton-like degradation of aromatic amines in textile dyeing sludge: Efficiency and mechanisms. *Environ. Sci. Pollut. Res.* **2019**, *26*, 7810–7820. [[CrossRef](#)] [[PubMed](#)]
158. Siddique, M.; Farooq, R.; Price, G.J. Synergistic effects of combining ultrasound with the Fenton process in the degradation of Reactive Blue 19. *Ultrason. Sonochemistry* **2014**, *21*, 1206–1212. [[CrossRef](#)] [[PubMed](#)]
159. Al, T.J.; Hossein, M.; Edris, K.; Ayat, B.; Panahi, H.; Fernandes, M. Optimization the effects of physicochemical parameters on the degradation of cephalixin in sono-Fenton reactor by using box-Behnken response surface methodology. *Catal. Lett.* **2019**, *149*, 1186–1196.
160. Ammar, H.B. Sono-Fenton process for metronidazole degradation in aqueous solution: Effect of acoustic cavitation and peroxydisulfate anion. *Ultrason. Sonochemistry* **2016**, *33*, 164–169. [[CrossRef](#)]
161. Dukkanci, M. Heterogeneous sonocatalytic degradation of bisphenol-A and the influence of the reaction parameters and ultrasonic frequency. *Water Sci. Technol.* **2019**, in press. [[CrossRef](#)]
162. Dinesh, G.K.; Chakma, S. Mechanistic investigation in degradation mechanism of 5-fluorouracil using graphitic carbon nitride. *Ultrason. Sonochemistry* **2019**, *50*, 311–321. [[CrossRef](#)]
163. Elshafei, G.M.S.; Yehia, F.Z.; Dimitry, O.I.H.; Badawi, A.M.; Eshaq, G. Ultrasonic assisted-Fenton-like degradation of nitrobenzene at neutral pH using nanosized oxides of Fe and Cu. *Ultrason. Sonochemistry* **2014**, *21*, 1358–1365. [[CrossRef](#)]
164. Lops, C.; Ancona, A.; Di, K.; Dumontel, B.; Garino, N. Sonophotocatalytic degradation mechanisms of Rhodamine B dye via radicals generation by micro- and nano-particles of ZnO. *Appl. Catal. B Environ.* **2019**, *243*, 629–640. [[CrossRef](#)] [[PubMed](#)]
165. Vaishnave, P.; Kumar, A.; Ameta, R.; Punjabi, P.B.; Ameta, S.C. Photo oxidative degradation of azure-B by sono-photo-Fenton and photo-Fenton reagents. *Arab. J. Chem.* **2012**, *7*, 981–985. [[CrossRef](#)]
166. Alekhina, M.B.; Khabirova, K.A.; Kon, T.V.; Prosvirin, I.P. Y-Type zeolites for the catalytic oxidative degradation of organic azo dyes in wastewater. *Kinet. Catal.* **2017**, *58*, 506–512. [[CrossRef](#)]
167. Taran, O.P.; Zagoruiko, A.N. Cu and Fe-containing ZSM-5 zeolites as catalysts for wet peroxide oxidation of organic contaminants: Reaction kinetics. *Res. Chem. Intermed.* **2015**, *41*, 9521–9537. [[CrossRef](#)]

168. Gupta, V.; Rakesh, M. Catalytic wet peroxide oxidation (CWPO) of 2-hydroxybenzoic acid and contaminated industrial effluent using LnMO_3 (Ln= La or Pr and M= Fe or Fe-Co). *J. Water Process Eng.* **2019**, *27*, 58–66. [[CrossRef](#)]
169. Shukla, P.; Wang, S.; Singh, K.; Ang, H.M.; Tadó, M.O. Cobalt exchanged zeolites for heterogeneous catalytic oxidation of phenol in the presence of peroxymonosulphate. *Appl. Catal. B, Environ.* **2010**, *99*, 163–169. [[CrossRef](#)]
170. Alekhina, M.B.; Papkova, M.V.; Kon, T.V.; Kutepov, B.I. Catalysts based on NaY zeolite for oxidative destruction of organic azo dyes in wastewater. *Russ. J. Appl. Chem.* **2013**, *86*, 1741–1745. [[CrossRef](#)]
171. Ilunga, A.K.; Meijboom, R. Catalytic oxidation of methylene blue by dendrimer encapsulated silver and gold nanoparticles. *J. Mol. Catal. A Chem.* **2015**, *411*, 48–60. [[CrossRef](#)]
172. Ncube, P.; Bingwa, N.; Baloyi, H.; Meijboom, R. Catalytic activity of palladium and gold dendrimer-encapsulated nanoparticles For methylene blue reduction: A kinetic analysis. *Appl. Catal. A Gen.* **2015**, *495*, 63–71. [[CrossRef](#)]
173. Ndolomingo, M.J.; Meijboom, R. Kinetic analysis of catalytic oxidation of methylene blue over $\gamma\text{-Al}_2\text{O}_3$ supported copper nanoparticles. *Appl. Catal. A Gen.* **2015**, *506*, 33–43. [[CrossRef](#)]
174. Naskar, S.; Pillay, S.A.; Chanda, M. Photocatalytic degradation of organic dyes in aqueous solution with TiO_2 nanoparticles immobilized on foamed polyethylene sheet. *J. Photochem. Photobiol. A Chem.* **1998**, *113*, 257–264. [[CrossRef](#)]
175. Salem, I.A.; El-maazawi, M.S. Kinetics and mechanism of color removal of methylene blue with hydrogen peroxide catalyzed by some supported alumina surfaces. *Chemosphere* **2000**, *41*, 1173–1180. [[CrossRef](#)]
176. Salem, I.A.; El-ghamry, H.A.; El-ghobashy, M.A. Catalytic decolorization of acid blue 29 dye by H_2O_2 and a heterogenous catalyst. *Beni-Suef Univ. J. Basic Appl. Sci.* **2014**, *3*, 186–192. [[CrossRef](#)]
177. Xaba, M.S.; Noh, J.; Meijboom, R. Catalytic activity of different sizes of $\text{Pt}/\text{Co}_3\text{O}_4$ in the oxidative degradation of Methylene Blue with H_2O_2 . *Appl. Surf. Sci.* **2018**, *467*, 868–880.
178. Amini, M.; Khaksar, M.; Ellern, A.; Woo, L.K. A new nanocluster polyoxomolybdate $[\text{Mo}_{36}\text{O}_{110}(\text{NO})_4(\text{H}_2\text{O})_{14}]\cdot 52\text{H}_2\text{O}$: Synthesis, characterization and application in oxidative degradation of common organic dyes. *Chin. J. Chem. Eng.* **2017**, *26*, 337–342. [[CrossRef](#)]
179. Javaid, R.; Kawanami, H.; Chatterjee, M.; Ishizaka, T. Fabrication of microtubular reactors coated with thin catalytic layer (M=Pd, Pd–Cu, Pt, Rh, Au). *Catal. Commun.* **2010**, *11*, 1160–1164. [[CrossRef](#)]
180. Javaid, R.; Yaqub, U.; Kawasaki, S. Highly efficient decomposition of remazol brilliant blue R using tubular reactor coated with thin layer of PdO. *J. Environ. Manag.* **2016**, *180*, 551–556. [[CrossRef](#)]
181. Jähnisch, K.; Hessel, V.; Löwe, H.; Baerns, M. Chemistry in microreactors; chemistry in microstructured reactors. *Angew. Chem. Int. Ed.* **2004**, *43*, 406–446. [[CrossRef](#)]
182. Kiwi-minsker, L.; Renken, A. Microstructured reactors for catalytic reactions. *Catal. Today* **2005**, *110*, 2–14. [[CrossRef](#)]
183. Kobayashi, J.; Mori, Y.; Okamoto, K.; Akiyama, R.; Ueno, M.; Kitamori, T.; Kobayashi, S. A microfluidic device for conducting gas-liquid-solid hydrogenation reactions. *Science* **2004**, *304*, 1305–1308. [[CrossRef](#)]
184. Kobayashi, J.; Mori, Y.; Kobayashi, S. Triphase hydrogenation reactions utilizing palladium-immobilized capillary column reactors and a demonstration of suitability for large scale synthesis. *Communication* **2005**, *347*, 1889–1892. [[CrossRef](#)]
185. Daskalaki, V.M.; Timotheatou, E.S.; Katsaounis, A.; Kalderis, D. Degradation of reactive red 120 using hydrogen peroxide in subcritical water. *Desalination* **2011**, *274*, 200–205. [[CrossRef](#)]
186. Daneshvar, S.; Salak, F.; Yoshida, H. Decomposition and decoloration of synthetic dyes using hot/liquid (subcritical) water. *Water Res.* **2010**, *44*, 1900–1908.
187. Akgu, M. Removal of C. I. basic blue 41 from aqueous solution by supercritical water oxidation in continuous-flow reactor. *J. Ind. Eng. Chem.* **2009**, *15*, 803–808.
188. Sogut, O.O.; Akgun, M. Treatment of dyehouse waste-water by supercritical water oxidation: A case study. *J. Chem. Technol. Biotechnol.* **2010**, *85*, 640–647. [[CrossRef](#)]
189. Javaid, R.; Kawasaki, S.; Ookawara, R.; Sato, K.; Nishioka, M.; Suzuki, A.; Suzuki, T.M. Continuous dehydrogenation of aqueous formic acid under sub-critical conditions by use of hollow tubular reactor coated with thin palladium oxide layer. *J. Chem. Eng. Jpn.* **2013**, *46*, 751–758. [[CrossRef](#)]
190. Javaid, R.; Kawanami, H.; Chatterjee, M.; Ishizaka, T. Sonogashira C–C coupling reaction in water using tubular reactors with catalytic metal inner surface. *Chem. Eng. J.* **2011**, *167*, 431–435. [[CrossRef](#)]

191. Javaid, R.; Qazi, U.Y.; Kawasaki, S. Efficient and continuous decomposition of hydrogen peroxide using a silica capillary coated with a thin palladium or platinum Layer. *Bull. Chem. Soc. Jpn.* **2015**, *88*, 976–980. [[CrossRef](#)]
192. Javaid, R.; Kawasaki, S.; Suzuki, A.; Suzuki, T.M. Simple and rapid hydrogenation of *p*-nitrophenol with aqueous formic acid in catalytic flow reactors. *Beilstein J. Org. Chem.* **2013**, *9*, 1156–1163. [[CrossRef](#)]
193. Javaid, R.; Tanaka, D.A.P.; Kawanami, H.; Suzuki, T.M. Silica capillary with thin metal (Pd and Pt) inner wall: Application to continuous decomposition of hydrogen peroxide. *Chem. Lett.* **2009**, *38*, 146–147. [[CrossRef](#)]
194. Akg, M.; Onur, O. Treatment of textile wastewater by SCWO in a tube reactor. *J. Supercrit. Fluids* **2007**, *43*, 106–111.
195. Bhargava, S.K.; Tardio, J.; Prasad, J.; Fo, K.; Akolekar, D.B.; Grocott, S.C. Wet oxidation and catalytic wet oxidation. *Ind. Eng. Chem. Res.* **2006**, *45*, 1221–1258. [[CrossRef](#)]
196. Voloshin, Y.; Manganaro, J.; Lawal, A. Kinetics and mechanism of decomposition of hydrogen peroxide over Pd/SiO₂ catalyst. *Ind. Eng. Chem. Res.* **2008**, *47*, 8119–8125. [[CrossRef](#)]
197. Choudhary, V.R.; Samanta, C.; Choudhary, T.V. Factors influencing decomposition of H₂O₂ over supported Pd catalyst in aqueous medium. *J. Mol. Catal. A Chem.* **2006**, *260*, 115–120. [[CrossRef](#)]
198. Hu, L.; Zhang, G.; Liu, M.; Wang, Q.; Dong, S.; Wang, P. Application of nickel foam-supported Co₃O₄-Bi₂O₃ as a heterogeneous catalyst for BPA removal by peroxymonosulfate activation. *Sci. Total Environ.* **2019**, *647*, 352–361. [[CrossRef](#)]
199. Hu, L.; Zhang, G.; Liu, M.; Wang, Q.; Wang, P. Optimization of the catalytic activity of a ZnCo₂O₄ catalyst in peroxymonosulfate activation for bisphenol A removal using response surface methodology. *Chemosphere* **2018**, *212*, 152–161. [[CrossRef](#)]
200. Hu, P.; Long, M. Cobalt-catalyzed sulfate radical-based advanced oxidation: A review on heterogeneous catalysts and applications. *Appl. Catal. B Environ.* **2016**, *181*, 103–117. [[CrossRef](#)]
201. Ghanbari, F.; Moradi, M. Application of peroxymonosulfate and its activation methods for degradation of environmental organic pollutants. *Chem. Eng. J.* **2017**, *310*, 41–62. [[CrossRef](#)]
202. Guerra-Rodr, S.; Rodriguez, E.; Singh, D.N.; Chueca, J.R. Assessment of sulfate radical-based advanced oxidation processes for water and wastewater treatment: A review. *Water* **2018**, *10*, 1828. [[CrossRef](#)]
203. Du, Y.; Ma, W.; Liu, P.; Zou, B.; Ma, J. Magnetic CoFe₂O₄ nanoparticles supported on titanate nanotubes (CoFe₂O₄/TNTs) as a novel heterogeneous catalyst for peroxymonosulfate activation and degradation of organic pollutants. *J. Hazard. Mater.* **2016**, *308*, 58–66. [[CrossRef](#)]
204. Oh, W.; Dong, Z.; Lim, T. Generation of sulfate radical through heterogeneous catalysis for organic contaminants removal: Current development, challenges and prospects. *Appl. Catal. B Environ.* **2016**, *194*, 169–201. [[CrossRef](#)]
205. Tan, C.; Gao, N.; Fu, D.; Deng, J.; Deng, L. Efficient degradation of paracetamol with nanoscaled magnetic CoFe₂O₄ and MnFe₂O₄ as a heterogeneous catalyst of peroxymonosulfate. *Sep. Purif. Technol.* **2016**, *175*, 47–57. [[CrossRef](#)]
206. Wang, H.; Lan, P. Enhancing the natural history awareness of lumbar disc displacement and facilitating rehabilitation following surgery. *Spine J.* **2018**, *18*, 2374–2375. [[CrossRef](#)] [[PubMed](#)]
207. Černík, M.; Dionysiou, D.D. Chemistry of persulfates in water and wastewater treatment: A review. *Chem. Eng. J.* **2017**, *330*, 44–62.
208. Wang, Z.; Yuan, R.; Guo, Y.; Xu, L.; Liu, J. Effects of chloride ions on bleaching of azo dyes by Co²⁺/oxone reagent: Kinetic analysis. *J. Hazard. Mater.* **2011**, *190*, 1083–1087. [[CrossRef](#)]
209. Taylor, P.; Shi, P. Supported Co₃O₄ on expanded graphite as a catalyst for the degradation of Orange II in water using sulfate radicals. *Des. Water Treat.* **2013**, *52*, 37–41.
210. Oh, W.; Chang, V.W.C.; Hu, Z.; Goei, R.; Lim, T. Enhancing the catalytic activity of gC₃N₄ through Me doping (Me=Cu, Co and Fe) for selective sulfathiazole degradation via redox based advanced oxidation process. *Chem. Eng. J.* **2017**, *323*, 260–269. [[CrossRef](#)]
211. Deng, L.; Shi, Z.; Zou, Z.; Zhou, S. Magnetic EDTA functionalized CoFe₂O₄ nanoparticles (EDTA-CoFe₂O₄) as a novel catalyst for peroxymonosulfate activation and degradation of orange G. *Environ. Sci. Pollut. Res.* **2017**, *24*, 11536–11548. [[CrossRef](#)]
212. Feng, Y.; Liu, J.; Wu, D.; Zhou, Z.; Deng, Y.; Zhang, T.; Shih, K. Efficient degradation of sulfamethazine with CuCo₂O₄ spinel nanocatalysts for peroxymonosulfate activation. *Chem. Eng. J.* **2015**, *280*, 514–524. [[CrossRef](#)]

213. Guo, T.; Wang, K.; Zhang, G.; Wu, X. A novel α -Fe₂O₃@g-C₃N₄ catalyst: Synthesis derived from Fe-based MOF and its superior photo-Fenton performance. *Appl. Surf. Sci.* **2018**, *469*, 331–339. [[CrossRef](#)]
214. Chen, Y.; Li, N.; Zhang, Y.; Zhang, L. Novel low-cost Fenton-like layered Fe-titanate catalyst: Preparation, characterization and application for degradation of organic colorants. *J. Colloid Interface Sci.* **2014**, *422*, 9–15. [[CrossRef](#)] [[PubMed](#)]
215. Wang, Q.; Tian, S.; Ning, P. Degradation mechanism of methylene blue in a heterogeneous Fenton-like reaction catalyzed by ferrocene. *Ind. Eng. Chem. Res.* **2014**, *53*, 643–649. [[CrossRef](#)]
216. Kavitha, V.; Palanivelu, K.Å. Destruction of cresols by Fenton oxidation process. *Water Res.* **2005**, *39*, 3062–3072. [[CrossRef](#)] [[PubMed](#)]
217. Xu, X.; Li, X.; Li, X.; Li, H. Degradation of melatonin by UV, UV/H₂O₂, Fe²⁺/H₂O₂ processes. *Sep. Purif. Technol.* **2009**, *68*, 261–266. [[CrossRef](#)]
218. Daud, N.K.; Ahmad, M.A.; Hameed, B.H. Decolorization of Acid Red 1 dye solution by Fenton-like process using Fe–Montmorillonite K10 catalyst. *Chem. Eng. J.* **2010**, *165*, 111–116. [[CrossRef](#)]
219. Ji, F.; Li, C.; Zhang, J.; Deng, L. Efficient decolorization of dye pollutants with LiFe (WO₄)₂ as a reusable heterogeneous Fenton-like catalyst. *Desalination* **2011**, *269*, 284–290. [[CrossRef](#)]
220. Zhao, W.G. Catalytic activity of MOF(2Fe/Co)/carbon aerogel for improving H₂O₂ and ·OH generation in solar photo–electro–Fenton process. *Appl. Catal. B Environ.* **2016**, *203*, 127–137. [[CrossRef](#)]
221. Shi, X.; Tian, A.; You, J.; Yang, H.; Wang, Y.; Xue, X. Degradation of organic dyes by a new heterogeneous Fenton reagent-Fe₂GeS₄ nanoparticle. *J. Hazard. Mater.* **2018**, *353*, 182–189. [[CrossRef](#)]
222. Salazar, L.M.; Grisales, C.M.; Garcia, D.P. How does intensification influence the operational and environmental performance of photo-Fenton processes at acidic and circumneutral pH. *Environ. Sci. Pollut. Res.* **2019**, *26*, 4367–4380. [[CrossRef](#)]
223. Zazo, J.A.; Pliego, G.; Blasco, S.; Casas, J.A.; Rodriguez, J.J. Intensification of the Fenton process by increasing the temperature. *Ind. Eng. Chem. Res.* **2011**, *50*, 866–870. [[CrossRef](#)]
224. Palaniandy, P.; Aziz, H.A.; Feroz, S. A review on the Fenton process for wastewater treatment. *J. Innov. Eng.* **2015**, *3*, 4–26.
225. Ertugay, N.; Acar, F.N. Removal of COD and color from direct blue 71 azo dye wastewater by Fenton's oxidation: Kinetic study. *Arab. J. Chem.* **2013**, *10*, S1158–S1163. [[CrossRef](#)]
226. Kushwaha, R.; Garg, S.; Bajpai, S.; Giri, A.S. Degradation of Nile blue sulphate dye onto iron oxide nanoparticles: Kinetic study, identification of reaction intermediates, and proposed mechanistic pathways. *Asia-Pac. J. Chem. Eng.* **2018**, *13*, e2200. [[CrossRef](#)]
227. Huang, R.; Fang, Z.; Yan, X.; Cheng, W. Heterogeneous sono-Fenton catalytic degradation of bisphenol A by Fe₃O₄ magnetic nanoparticles under neutral condition. *Chem. Eng. J.* **2012**, *197*, 242–249. [[CrossRef](#)]
228. Tian, S.H.; Tu, Y.T.; Chen, D.S.; Chen, X.; Xiong, Y. Degradation of acid orange II at neutral pH using Fe₂(MoO₄)₃ as a heterogeneous Fenton-like catalyst. *Chem. Eng. J.* **2011**, *169*, 31–37. [[CrossRef](#)]
229. Dulman, V.; Cucu-man, S.M.; Iulian, R.; Buhaceanu, R. A new heterogeneous catalytic system for decolorization and mineralization of orange G acid dye based on hydrogen peroxide and a macroporous chelating polymer. *Dyes Pigments* **2012**, *95*, 79–88. [[CrossRef](#)]
230. Hassan, H.; Pauh, P.; Pinang, P. Decolorization of acid red 1 by heterogeneous Fenton-like reaction using Fe-ball clay catalyst. In *International Conference on Environment Science and Engineering*; IACSIT Press: Singapore, 2011; Volume 8, pp. 232–236.
231. Blaney, L.; Lawler, D.F.; Katz, L.E. Transformation kinetics of cyclophosphamide and ifosfamide by ozone and hydroxyl radicals using continuous oxidant addition reactors. *J. Hazard. Mater.* **2018**, *364*, 752–761. [[CrossRef](#)] [[PubMed](#)]
232. Salem, I.A.; El-ghamry, H.A.; Ghobashy, M.A.E. Application of montmorillonite–Cu(II)ethylenediamine catalyst for the decolorization of Chromotrope 2R with H₂O₂ in aqueous solution. *Spectrochim. Acta. A* **2015**, *139*, 130–137. [[CrossRef](#)] [[PubMed](#)]

233. Mohajeri, S.; Aziz, H.A.; Isa, M.H.; Bashir, M.J.K.; Mohajeri, L.; Adlan, M.N. Influence of Fenton reagent oxidation on mineralization and decolorization of municipal landfill leachate. *J. Environ. Sci. Health. A Tox. Hazard. Subst. Environ. Eng.* **2010**, *45*, 692–698. [[CrossRef](#)] [[PubMed](#)]
234. Karthikeyan, S.; Titus, A.; Gnanamani, A.; Mandal, A.B.; Sekaran, G. Treatment of textile wastewater by homogeneous and heterogeneous Fenton oxidation processes. *Desalination* **2011**, *281*, 438–445. [[CrossRef](#)]



© 2019 by the authors. Licensee MDPI, Basel, Switzerland. This article is an open access article distributed under the terms and conditions of the Creative Commons Attribution (CC BY) license (<http://creativecommons.org/licenses/by/4.0/>).